Published version in IEEE Transactions on Robotics
Vol. 33, Issue 6, Dec. 2017
DOI: 10.1109/TRO.2017.2750697

Invariance Control for Safe Human-Robot Interaction in Dynamic Environments

Melanie Kimmel, *Student Member, IEEE,* Sandra Hirche, *Senior Member, IEEE,*

***Abstract*—In human-robot interaction, it is essential to ensure that the robot poses no threat to the human. Especially in applications which require close or physical interaction, e.g. collaborative manufacturing or rehabilitation, the danger emanating from the robot has to be minimized. Control schemes introducing virtual constraints have proven valuable in this context since they allow to define a safe zone to move in without endangering the human. Combining the different requirements on the control scheme such as real-time capability, stability, and reliability in the presence of external disturbances and dynamic limits, however, turns out to be challenging. In this article, we present a novel control scheme for human-robot interaction, which enforces dynamic constraints even in the presence of external forces. Based on an analytic constraint description and a feedback linearization of the system dynamics, a safe set of states is determined which is then rendered controlled positively invariant thus keeping the system in a safe configuration. The controlled system is analyzed with respect to invariance and boundedness with the results being illustrated in a full-scale experiment.**

***Index Terms*—Invariance control, human-robot interaction, collision avoidance, safety, real-time systems, motion control, nonlinear dynamical systems, time-varying systems, lyapunov methods.**

I. Introduction

Capabilities of robotic systems have considerably improved over the past years and the development of dexterous grippers, omni-directional platforms and strong manipulators has opened up many fields of application. These new systems are potential assistants in health care and rehabilitation, possibly even as wearable devices. Exoskeletons help patients with motor disorders [1] and mobile robots take over tasks in domestic and industrial environments [2], [3]. This expansion of application domains introduces new challenges to the control of the robotic systems especially with respect to meeting fundamental safety requirements as stated in [4], [5].

Depending on the field of application, the robot has to carry out a specific task. This is achieved by an approach with explicit goal description such as PD (proportional-derivative) tracking control [6] and impedance control [7] or with implicit goal description such as reinforcement learning strategies [8], [9]. Since damage to the robot and its surroundings must be avoided, constraints imposed by the environment as well as joint and velocity limits have to be enforced. Especially for tasks, which involve close or even physical interaction with humans, the most important issue is to keep any humans in the vicinity of the robot safe at all times. As humans move and everyday environments often change dynamically, the constraints vary over time, which requires the applied constraint enforcing control scheme to deal with such time-dependency. An appropriate control action has to be determined in real-time to guarantee constraint adherence. However, even in the presence of constraints, the robot should be able to use as much of the unconstrained state space as possible for achieving the task objective. This means that the control scheme, which is responsible for enforcing the constraints, should not restrict the manipulator more than absolutely necessary. This is especially important in narrow and cluttered environments, where it is essential to use as much of the available space as possible. Additionally, physical interaction with humans causes interaction forces to act on the robot. These forces need to be accounted for in the control scheme and must not lead to a violation of a constraint. To summarize, a control scheme, which may be used for applications including close and physical human-robot interaction, has to reliably provide constraint enforcing control in real-time. The system should follow the control goal using the available space while guaranteeing adherence to dynamic constraints even in the presence of external disturbances.

Currently available control schemes strongly enforce some of these requirements but are challenged when it comes to others. Since it is important to address all the introduced aspects, this generates the necessity for a control scheme, which reliably meets all the challenges of safety in close and physical human-robot interaction.

All authors are with the Chair of Information-Oriented Control, Department of Electrical and Computer Engineering, Technical University of Munich, D-80290 München, Germany. {melanie.kimmel, hirche}@tum.de

A. Contribution

In this work, we introduce a novel control scheme for robotic systems, which is able to guarantee state and output constraint enforcement. The proposed invariance control scheme has the advantage of being implemented in addition to an existing control law, which is designed according to performance specifications and the control goal of the system. As a result, invariance control is applicable in many scenarios and applications, where constraints have to be added to an existing control structure. In order to keep the system constraint admissible, a method is provided to determine an admissible subset in state space based on the given constraints and the system dynamics. Invariance control is able to deal with a variety of constraints, including joint, velocity and workspace constraints and even dynamic constraints, e.g. to account for moving humans in the vicinity. We formally show that the designed control scheme keeps the system within the admissible subset for all times while keeping the tracking error with respect to the original desired trajectory bounded. This is also true in the presence of external (input) disturbances. To illustrate the fact that the control scheme presents a solution for scenarios including physical contact of robots and humans, we conduct an experimental evaluation on a real robotic platform.

B. Related Work

Naturally, there are various other well-known control schemes addressing the issue of enforcing constraints. One approach is model-predictive control (MPC) [10]. The optimization-based approach allows for input, output and state constraints. For high-dimensional and nonlinear systems and a high number of constraints, the computational cost may, however, prevent the execution in real-time. Another optimization-based approach is the reference governor [11], which is the base for many approaches such as command governors [12] or fast reference governors [13]. Allowing for system disturbances, these approaches are designed for discrete-time systems and, similar to MPC, real-time requirements may not be met due to the required numerical simulation. Control based on barrier certificates [14] and functions [15], [16] on the other hand does not require extensive optimization and allows for the definition of soft and hard constraints on the system while combining them with control objectives. It does, however, not provide solutions in case of constraint violation, which may lead to instability and undesired behavior. Methods, which provide a trade-off between reaching the control objective and keeping the system safe, are also found in shared control [17]. The result is, however, a system which does not use the safe space to all extent. Finally, there are the widely used collision avoidance approaches for robotic systems such as potential fields [18], the dynamic window approach [19], virtual wall rendering [20] and virtual fixtures [21], which do not explicitly take the system dynamics into account. As the system dynamics are not negligible especially

Published version in IEEE Transactions on Robotics
Vol. 33, Issue 6, Dec. 2017
DOI: 10.1109/TRO.2017.2750697

for high inertias or high accelerations, these approaches are unable to guarantee the adherence to the constraints.

The concept of invariance control is introduced in [22] for nonlinear, control affine single-input single-output (SISO) systems. Implementation in addition to a nominal control law is introduced in [23] and an extension to multi-input multi-output (MIMO) systems is provided in [24]. The issue of chattering, which is a result of a sampled data implementation, is addressed in [25]. Invariance control is successfully applied to control legged robots [26] and to enforce 6D workspace constraints [27]. In preliminary work of the authors, an invariance control scheme for the use with time-varying constraints is developed [28] and evaluated experimentally on an anthropomorphic manipulator [29]. The influence of constraint violation and external disturbances on the control performance is, however, not discussed. Additionally, conclusive proof of invariance and boundedness of an invariance controlled robotic system is missing to date.

C. Notation

By convention, vectors are denoted by bold small characters, matrices by bold capital characters. The Euclidean vector norm (2-norm) of a vector $\boldsymbol{x} \in \mathbb{R}^n$ is written as $\|\boldsymbol{x}\|_2 = \sqrt{\boldsymbol{x}^\intercal \boldsymbol{x}}$. The expression $\boldsymbol{x}_1 \preccurlyeq \boldsymbol{x}_2$ indicates the element-wise inequality of two vectors $\boldsymbol{x}_1, \boldsymbol{x}_2 \in \mathbb{R}^n$. Stacking scalars or vectors to receive a vector or a matrix, respectively, is denoted by square brackets

$$\boldsymbol{A} = [\boldsymbol{a}_i^\intercal] = \begin{bmatrix} \boldsymbol{a}_1^\intercal \\ \vdots \\ \boldsymbol{a}_k^\intercal \end{bmatrix} \in \mathbb{R}^{k \times n} , \quad \boldsymbol{b} = [b_i] = \begin{bmatrix} b_1 \\ \vdots \\ b_k \end{bmatrix} \in \mathbb{R}^{k \times 1} .$$

Low order time derivatives are indicated by dots $\dot{x} = \frac{\mathrm{d}x}{\mathrm{d}t}$, higher order time derivatives by superscripts $x^{(k)} = \frac{\mathrm{d}^k x}{\mathrm{d}t^k}$. The first order Lie derivative, i.e. the directional derivative in direction $\boldsymbol{f}$ of a scalar function $h(\boldsymbol{x})$, is given by

$$\mathcal{L}_{\boldsymbol{f}} h(\boldsymbol{x}) = \frac{\partial h}{\partial \boldsymbol{x}} \boldsymbol{f} .$$

Lie derivatives of higher order $\mathcal{L}_{\boldsymbol{f}}^i h(\boldsymbol{x})$, $i > 1$ are determined recursively. The set of k times continuously differentiable functions $\boldsymbol{h} : \mathbb{R}^n \to \mathbb{R}^m$ is denoted by $\mathcal{C}^k(\mathbb{R}^m, \mathbb{R}^n)$. The system parts are identified by corresponding subscripts. The subscript 'des' refers to the desired system action, 'no' to nominal control, 'c' to the control input of the torque controlled robot, 'ext' to external disturbances, 'm' to the torque controller, 'q' to joint space and 'p' indicates the task space.

II. Constrained Robotic System

Safe human-robot interaction requires compliance with safety relevant constraints, thus causing the need for a control scheme, which is able to guarantee compliance with these limits. This section introduces the general dynamic model of the robotic system and the requirements imposed upon the constraint description and a nominal control scheme for unconstrained task execution such that a constraint enforcing control scheme may be designed.

A. Robotic system equations

For the robotic system, we consider the general dynamics

$$\boldsymbol{M}_{\boldsymbol{q}}(\boldsymbol{q})\ddot{\boldsymbol{q}} + \boldsymbol{C}_{\boldsymbol{q}}(\boldsymbol{q}, \dot{\boldsymbol{q}})\dot{\boldsymbol{q}} + \boldsymbol{g}_{\boldsymbol{q}}(\boldsymbol{q}) = \boldsymbol{\tau} \tag{1}$$

where $\boldsymbol{q}(t) \in \mathbb{R}^{n_q}$ are generalized coordinates, $\boldsymbol{M}_{\boldsymbol{q}}(\boldsymbol{q}) \in \mathbb{R}^{n_q \times n_q}$ is the mass matrix, $\boldsymbol{C}_{\boldsymbol{q}}(\boldsymbol{q}, \dot{\boldsymbol{q}})\dot{\boldsymbol{q}} \in \mathbb{R}^{n_q}$ are the Coriolis and centripetal forces, $\boldsymbol{g}_{\boldsymbol{q}}(\boldsymbol{q}) \in \mathbb{R}^{n_q}$ the gravitational torques and $\boldsymbol{\tau} \in \mathbb{R}^{n_q}$ is the input torque of the system. The dynamics represent the reaction of a robotic system to the applied actuator torques $\boldsymbol{\tau}$, which consist of the control torques $\boldsymbol{\tau}_\mathrm{m} \in \mathbb{R}^{n_q}$, the external input disturbances $\boldsymbol{\tau}_\mathrm{ext} \in \mathbb{R}^{n_q}$ and torques $\boldsymbol{\tau}_\mathrm{e} \in \mathbb{R}^{n_q}$ resulting from measurement errors and unmodeled dynamics

$$\boldsymbol{\tau} = \boldsymbol{\tau}_\mathrm{m} + \boldsymbol{\tau}_\mathrm{ext} + \boldsymbol{\tau}_\mathrm{e} . \tag{2}$$

The external disturbances are a result of the physical interaction with the human and the environment. Any physical contact with a human or the environment generates contact forces and torques, which translate into disturbance joint torques. These external forces may be either desired and included in a nominal control scheme or undesired, for example as a result from an unexpected collision.

In the following, for notational convenience, the explicit dependency on $\boldsymbol{q}$ and $\dot{\boldsymbol{q}}$ of the matrices $\boldsymbol{M}_{\boldsymbol{q}}(\boldsymbol{q})$ and $\boldsymbol{C}_{\boldsymbol{q}}(\boldsymbol{q}, \dot{\boldsymbol{q}})$ as well as of the vector $\boldsymbol{g}_{\boldsymbol{q}}(\boldsymbol{q})$ will be omitted. The states $\boldsymbol{q}$ and $\dot{\boldsymbol{q}}$ are concatenated in the vector $\boldsymbol{x}^\intercal = [\boldsymbol{q}^\intercal \, \dot{\boldsymbol{q}}^\intercal]^\intercal$.

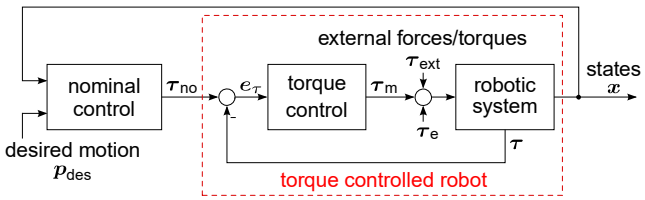

Fig. 1: Structure of the control loop of a torque-controlled robotic system under nominal control.

B. Robot control

The control scheme for torque-controlled robotic manipulators consists of two control loops as depicted in Fig. 1. The outer control loop with the nominal control law is designed to generate a control torque $\boldsymbol{\tau}_\mathrm{no} \in \mathbb{R}^{n_q}$, which enforces the desired behavior of the manipulator. The inner control loop with the torque controller ensures that the robot behaves according to the desired torques and compensates the effects of disturbance torques $\boldsymbol{\tau}_\mathrm{ext} \in \mathbb{R}^{n_q}$ and $\boldsymbol{\tau}_\mathrm{e} \in \mathbb{R}^{n_q}$.

Remark 1. *In the following, the control approach is introduced for torque-controlled robotic systems. However, by adapting the control law accordingly, it is readily applicable to position-controlled robots as well. In that case, the influence of disturbances and modeling errors need to be expressed in terms of the position error.*

The design of the torque control law in the inner loop is often based on the concept of passivity, leading to a PD control law [30]. The torque error

$$\boldsymbol{e}_\tau = \boldsymbol{\tau}_\mathrm{no} - \boldsymbol{\tau} \tag{3}$$

serves as the control input. In order to achieve $\boldsymbol{\tau} = \boldsymbol{\tau}_\mathrm{no} \in \mathbb{R}^{n_q}$ we make the following assumption on the torque control law.

Assumption 1. *The torque control loop is input-to-state stable with respect to bounded inputs $\boldsymbol{\tau}_{ext}$ and $\boldsymbol{\tau}_e$, i.e.*

$$\|\boldsymbol{e}_\tau(t)\| \leq \alpha(\|\boldsymbol{e}_\tau(t_0)\|, t - t_0) + \beta\left(\sup_{t_0 \leq s \leq t} \left\| \begin{bmatrix} \boldsymbol{\tau}_{ext}(s) \\ \boldsymbol{\tau}_e(s) \end{bmatrix} \right\|\right)$$

with a class $\mathcal{KL}$ function α and a class $\mathcal{K}$ function β holds for any initial error $\boldsymbol{e}_\tau(t_0)$ and all $t \geq t_0$.

The control goal of the outer loop is given by the interaction task and is defined in task coordinates $\boldsymbol{p} \in \mathbb{R}^{n_p}$, which are determined as a function $\boldsymbol{f}_{\boldsymbol{p}} : \mathbb{R}^{n_q} \to \mathbb{R}^{n_p}$ of the generalized coordinates

$$\boldsymbol{p} = \boldsymbol{f}_{\boldsymbol{p}}(\boldsymbol{q}) . \tag{4}$$

Published version in IEEE Transactions on Robotics
Vol. 33, Issue 6, Dec. 2017
DOI: 10.1109/TRO.2017.2750697

The Jacobian $\boldsymbol{J}(\boldsymbol{q}) = \frac{\partial \boldsymbol{p}}{\partial \boldsymbol{q}} \in \mathbb{R}^{n_p \times n_q}$ determines the relation between task space and joint velocities as well as between task space forces/torques $\boldsymbol{f} \in \mathbb{R}^{n_p}$ and joint torques

$$\dot{\boldsymbol{p}} = \boldsymbol{J}(\boldsymbol{q})\dot{\boldsymbol{q}} \tag{5}$$
$$\boldsymbol{\tau} = \boldsymbol{J}(\boldsymbol{q})^\intercal \boldsymbol{f} \ . \tag{6}$$

A well-known control law in physical human-robot interaction with torque-controlled manipulators is impedance control [7]. It imitates spring damper behavior with respect to a desired trajectory in reaction to measured or estimated external forces and torques. As a result, the robot carries out a desired motion, which may be actively changed by the human applying forces, since the robot reacts compliantly. Both the implementation in task coordinates [7] and in joint coordinates [31] are commonly used. For impedance control in task space, the control torque $\boldsymbol{\tau}_{\text{no}}$ is given by

$$\begin{aligned}\boldsymbol{\tau}_{\text{no}} = \boldsymbol{J}(\boldsymbol{q})^\intercal(\boldsymbol{f}_{\text{ext}} + \boldsymbol{M}_p\ddot{\boldsymbol{p}}_{\text{des}} + \boldsymbol{D}_p(\dot{\boldsymbol{p}}_{\text{des}} - \dot{\boldsymbol{p}}) + \boldsymbol{K}_p(\boldsymbol{p}_{\text{des}} - \boldsymbol{p})) \\ + \boldsymbol{C}_q(\boldsymbol{q}, \dot{\boldsymbol{q}})\dot{\boldsymbol{q}} + \boldsymbol{g}_q(\boldsymbol{q})\end{aligned} \tag{7}$$

with a sufficiently smooth desired trajectory $\boldsymbol{p}_{\text{des}}$, and the positive definite Cartesian mass $\boldsymbol{M}_p \in \mathbb{R}^{n_p \times n_p}$, stiffness $\boldsymbol{K}_p \in \mathbb{R}^{n_p \times n_p}$ and damping $\boldsymbol{D}_p \in \mathbb{R}^{n_p \times n_p}$ matrices. External forces $\boldsymbol{f}_{\text{ext}} \in \mathbb{R}^{n_p}$ are connected to the external torque $\boldsymbol{\tau}_{\text{ext}}$ by (6). The stiffness and damping parameters may be adapted, sometimes even on-line, to account for task requirements [32].

In order to guarantee safe and predictable cooperation, the control law has to be designed carefully to comply with the desired task specification and performance goal.

Assumption 2. *In the absence of external forces, i.e.* $\boldsymbol{f}_{ext} = \boldsymbol{0}$*, the continuous nominal control law globally stabilizes the tracking error* $\boldsymbol{e} = \boldsymbol{x}_{des}(t) - \boldsymbol{x}$ *in the sense of Lyapunov for a sufficiently smooth desired state trajectory* $\boldsymbol{x}_{des}(t)$*.*

This assumption ensures the tracking performance. It is generally fulfilled for control schemes with explicit goal descriptions, as here stability is the most basic design goal. For control schemes with implicit goal descriptions such as learning approaches, the stability assumption is not immediately clear. However, if the set of control laws, over which the learning is conducted, solely consists of stabilizing control laws, stable tracking is achieved.

Remark 2. *Assumption 2 is necessary to investigate boundedness in the following sections. In the presence of external forces or if boundedness is a subordinate control goal, the assumption may be disregarded as it does not influence the guarantees for constraint adherence. This means that other stability notions may be used, which is, however, not discussed further as the nominal control design is not within the scope of this work.*

In the following, constraint-enforcing measures are introduced, which avoid a violation of the constraints even in the presence of external forces. Note that as torque control uses the torque error as a control input, it is no restriction to assume that it is available for use in invariance control.

C. Constraints

For human-robot interaction, an accurate definition of the safety constraints, such as position and velocity constraints, is crucial to ensure operation consistent with the standards in [4], [5]. The constraints may be given by joint or velocity limits inherent in the robotic structure and a violation might lead to unexpected and unsafe motion. Additionally, obstacles and interacting humans impose workspace constraints. The shape of the constraint is determined by the geometrical properties of the obstacles. Upper or lower limits are usually best described by linear functions, whereas humans or more complex objects may be encased in multiple spherical constraints [33]. While the structural constraints will mostly be static, the environment may vary over time, since humans and obstacles might be moving. Therefore, similar to other model-based approaches such as MPC, a prediction-based representation of the constraints, which accounts for their dynamic nature, is required. This may be achieved by exploiting prior knowledge about the underlying dynamics, e.g. the minimum jerk properties of human motion [34], or by using a learning approach as e.g. in [2].

We model each constraint i by an analytic function $h_i(\boldsymbol{x}, \boldsymbol{\eta}(t))$, which depends on the system states $\boldsymbol{x}$ and a set of dynamic parameters $\boldsymbol{\eta}(t)$. Naturally, the parameters $\boldsymbol{\eta}(t)$ may be set at a constant value to model static constraints. The function provides a measure for the distance of the system from the constraint. It is equal to zero on the constraint, negative for admissible states and positive for inadmissible states. The set of l time-varying constraints is then specified by a vector of constraint functions

$$\boldsymbol{h}(\boldsymbol{x}, \boldsymbol{\eta}(t)) = \begin{bmatrix} h_1(\boldsymbol{x}, \boldsymbol{\eta}(t)) \\ \vdots \\ h_l(\boldsymbol{x}, \boldsymbol{\eta}(t)) \end{bmatrix} \ , \tag{8}$$

which depends on the system states $\boldsymbol{x}(t) = [\boldsymbol{q}^\intercal, \dot{\boldsymbol{q}}^\intercal]^\intercal \in \mathbb{R}^{2n_q}$ and the parameters $\boldsymbol{\eta}(t) \in \mathbb{R}^{n_\eta}$. They are considered an (artificial) output

$$\boldsymbol{y} = \boldsymbol{h}(\boldsymbol{x}, \boldsymbol{\eta}(t)) \tag{9}$$

of the robotic system, which is used in the derivation of a control scheme. Additionally, (8) defines the time-varying admissible set

$$\mathcal{H}(t) = \{\boldsymbol{x} \in \mathbb{R}^{2n_q} \,|\, h_i(\boldsymbol{x}(t), \boldsymbol{\eta}(t)) \leq 0 \quad \forall\, 1 \leq i \leq l\} \ . \tag{10}$$

In order to guarantee safe interaction, a corrective control law should guarantee compliance with the constraints, thus keeping the states of (1) within the admissible set for all times.

Assumption 3. *For all instants of time* t *and a sufficiently large constant* r_i *each constraint in the output* (9) *and the corresponding admissible set fulfill the following conditions:*

(i) Each element $\eta_j(t)$*,* $1 \leq j \leq n_\eta$ *is measurable and generated by possibly unknown stable underlying dynamics such that the parameter function is a* $\mathcal{C}^{r_i}$ *function with respect to time,*
(ii) each $\eta_j(t)$*,* $1 \leq j \leq n_\eta$ *and its* r_i *derivatives are bounded,*
(iii) each output function (9) *is a* $\mathcal{C}^{r_i}$ *function with respect to time,*
(iv) $\mathcal{H}(t)$ *is connected and* $\mathcal{H}(t) \neq \emptyset$*.*

Note that constraint dynamics, given by human motion, typically fulfill condition (i), as human motion is found to be jerk controlled [34]. Otherwise it may be achieved by approximating the parameters by a sufficiently smooth signal. If the parameters $\eta_j(t)$ are not measurable, they need to be estimated, e.g. by using an observer. Condition (iii) is ensured by designing the constraint function accordingly. It allows the robotic system to follow the dynamics of the constraint if necessary. Condition (iv) is a natural assumption, since it is only possible for the controlled system to remain constraint admissible if such states exist.

Note that the notion of the admissible set may be extended to multiple disjoint admissible sets $\mathcal{H}(t) = \mathcal{H}_1(t) \cup \ldots \cup \mathcal{H}_n(t)$, each $\mathcal{H}_i(t)$ defined by a set of constraints, cf. (10). In this case, constraint adherence may only be achieved if the set $\mathcal{H}_i(t)$ containing the initial system state fulfills Assumption 3. In the following, a computationally efficient control scheme, which combines task execution with a guaranteed constraint adherence is introduced.

Published version in IEEE Transactions on Robotics
Vol. 33, Issue 6, Dec. 2017
DOI: 10.1109/TRO.2017.2750697

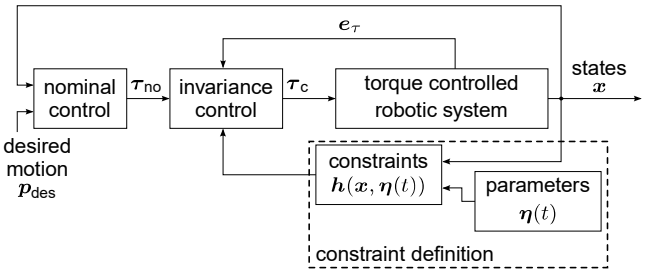

Fig. 2: Structure of the control loop of a robotic system controlled by a nominal controller combined with invariance control for safety.

III. Invariance control

Invariance control is a control scheme, which may be implemented as an add-on to any existing nominal control. It ensures that the system performs according to the desired behavior generated by nominal control within the admissible, i.e. safe, set. At the same time, it monitors the system motion towards the constraints and provides corrective control action, when it is necessary to avoid the violation of a constraint.

The structure of an invariance controlled robotic system is shown in Fig. 2. The states $\boldsymbol{x}$ of the robotic system (1) and the information about the desired system behavior $\boldsymbol{p}_{\text{des}}$ are used to determine the nominal control input $\boldsymbol{\tau}_{\text{no}}$. Invariance control combines (9) with $\boldsymbol{\tau}_{\text{no}}$ and calculates a corrective control input $\boldsymbol{\tau}_{\text{c}}$, which is as close as possible to $\boldsymbol{\tau}_{\text{no}}$ and avoids any violation of the constraints.

In the following, we will give a thorough introduction and analysis of invariance control with dynamic constraints in robotic applications. Invariance control usually assumes an ideal torque controlled robot, i.e. $\boldsymbol{e}_\tau = \boldsymbol{0}$. External forces, however, lead at least temporarily to a torque error $\boldsymbol{e}_\tau$ different from zero. Therefore, we will explicitly include the effects of a torque error in the control scheme. Invariance control is introduced for MIMO systems but application to systems with single input and/or single output is straightforward.

Invariance control is applicable to nonlinear, control affine MIMO systems [24]. The torque-controlled robotic system as shown in Fig. 1 has the input $\boldsymbol{\tau}_{\text{c}}$ and the states $\boldsymbol{x} = [\boldsymbol{q}^\intercal, \dot{\boldsymbol{q}}^\intercal]^\intercal \in \mathbb{R}^{2n_q}$. The system equations of the torque controlled robot

$$\underbrace{\begin{bmatrix}\dot{\boldsymbol{q}}\\ \ddot{\boldsymbol{q}}\end{bmatrix}}_{\dot{\boldsymbol{x}}} = \underbrace{\begin{bmatrix}\dot{\boldsymbol{q}}\\ -\boldsymbol{M_q}^{-1}\left(\boldsymbol{C_q}\dot{\boldsymbol{q}} + \boldsymbol{g_q}\right)\end{bmatrix}}_{\boldsymbol{f}(\boldsymbol{x})} + \underbrace{\begin{bmatrix}\boldsymbol{0}\\ \boldsymbol{M_q}^{-1}\end{bmatrix}}_{\boldsymbol{G}(\boldsymbol{x})=[\boldsymbol{g}_1(\boldsymbol{x})\ldots\boldsymbol{g}_{n_q}(\boldsymbol{x})]}\left(\boldsymbol{\tau}_{\text{c}} - \boldsymbol{e}_\tau\right) \tag{11}$$

are derived using (1) and (3) and show that the torque-controlled robotic system is, in fact, control affine with respect to the input $\boldsymbol{\tau}_{\text{c}}$. Based on these system equations, we will determine a corrective control input, which achieves adherence to the constraints in the presence of external forces/torques $\boldsymbol{\tau}_{\text{ext}}$ and torques caused by model and measurement uncertainties $\boldsymbol{\tau}_{\text{e}}$. With a proper design of the underlying torque control scheme, which is not part of this work, the resulting torque error $\boldsymbol{e}_\tau$ is bounded if the disturbance signals are bounded as well, which is usually the case for occurring disturbance torques $\boldsymbol{\tau}_{\text{ext}}$, $\boldsymbol{\tau}_{\text{e}}$ in a properly modeled robotic system.

Assumption 4. *The torque error is measurable and absolutely bounded,* $\|\boldsymbol{e}_\tau\|_2 \leq \delta_{e_\tau}$.

This assumption is required to be able to include the torque error in the control derivation.

Remark 3. *Since the torque error is the input to torque control, it is no restriction to assume its availability for invariance control.*

In the following, invariance control is introduced for constraints, which have relative degree one or two with respect to the system (11) as these are the most relevant in robotic applications. Nevertheless, invariance control is able to enforce constraints with a higher relative degree by adjusting the invariance function and the conditions. For more information, the interested reader is referred to [23].

A. Input-output-linearization

A violation of the constraints may only be avoided, if the influence of the control input on the motion towards a constraint is clear. Input-output (I/O)-linearization is a useful tool to determine the influence of the system input $\boldsymbol{\tau}_{\text{c}}$ on the output functions (9). It transforms the original system into an integrator chain with the same output and a new pseudo input, which is determined by the linearizing transformation. In the following, we show how the resulting linear system allows the definition of the instant of time, when a corrective action for constraint adherence is required and how the inverse transformation yields the required corrective control input. These derivations would become much harder, if not impossible, to solve without the use of the linearizing transformation.

In general, the I/O-linearization with respect to $y_i = h_i(\boldsymbol{x}, \boldsymbol{\eta}(t))$ transforms the system (11) with $2n_q$ states into an integrator chain and internal dynamics. The relation between the input $\boldsymbol{\tau}_{\text{c}}$ and the so-called pseudo input z_i of the integrator chain is determined by

$$z_i = y_i^{(r_i)} = \boldsymbol{a}_i^\intercal(\boldsymbol{x}, \boldsymbol{\eta}(t))\boldsymbol{\tau}_{\text{c}} + b_i(\boldsymbol{x}, \boldsymbol{\eta}(t), \ldots, \boldsymbol{\eta}^{(r_i)}(t)) \ , \tag{12}$$

with the relative degree r_i,

$$\begin{aligned}
&\boldsymbol{a}_i^\intercal(\boldsymbol{x}, \boldsymbol{\eta}(t)) = \left[\mathcal{L}_{\boldsymbol{g}_1}\mathcal{L}_{\boldsymbol{f}}^{r_i-1}y_i \ldots \mathcal{L}_{\boldsymbol{g}_m}\mathcal{L}_{\boldsymbol{f}}^{r_i-1}y_i\right] \neq \boldsymbol{0}^T \ ,\\
&\left[\mathcal{L}_{\boldsymbol{g}_1}\mathcal{L}_{\boldsymbol{f}}^{r-1}y_i \ldots \ \mathcal{L}_{\boldsymbol{g}_m}\mathcal{L}_{\boldsymbol{f}}^{r-1}y_i\right] = \boldsymbol{0}^T \quad \forall\, r < r_i \ ,\\
&b_i(\boldsymbol{x}, \boldsymbol{\eta}(t), \ldots, \boldsymbol{\eta}^{(r_i)}(t)) = \bar{\mathcal{L}}_{\boldsymbol{f}}^{r_i} y_i \ .
\end{aligned}$$

and the Lie operator including the dynamic parameters

$$\bar{\mathcal{L}}_{\boldsymbol{f}}^{r_i} y_i = \left(\frac{\partial}{\partial \boldsymbol{\eta}}(\cdot)\dot{\boldsymbol{\eta}} + \ldots + \frac{\partial}{\partial \boldsymbol{\eta}^{(r_i-1)}}(\cdot)\boldsymbol{\eta}^{(r_i)} + \mathcal{L}_{\boldsymbol{f}}\right)^{r_i} y_i \ . \tag{13}$$

Time-varying I/O-linearization yields a well-defined relative degree r_i of y_i, if $\boldsymbol{a}_i^\intercal(\boldsymbol{x}, \boldsymbol{\eta}(t)) \neq \boldsymbol{0}$ holds [35].

Assumption 5. *The vector* $\boldsymbol{a}_i^\intercal(\boldsymbol{x}, \boldsymbol{\eta}(t))$ *has at least one non-zero element for all instants of time, i.e.* $\boldsymbol{a}_i^\intercal(\boldsymbol{x}, \boldsymbol{\eta}(t)) \neq \boldsymbol{0}\, \forall t \geq 0$.

In view of the application, the constraints have to be designed such that the admissible set does not include any singularities as these lead to a loss of manipulability and unsafe behavior. Without any singularities in the admissible set, controllability is achieved and Assumption 5 holds. Intuitively, this means that it is possible to apply input torques which result in a motion away from the constraint.

As the constraints may introduce limits on all states of the robotic system, the corresponding output function $h_i(\boldsymbol{x}, \boldsymbol{\eta}(t))$ may depend solely on the joints $\boldsymbol{q}$, solely on $\dot{\boldsymbol{q}}$ or on all states. Since the form of the output function determines the relative degree, we now examine the I/O-linearization with respect to two types of output functions: full state output functions $y_i = h_i(\boldsymbol{x}, \boldsymbol{\eta}(t))$ depending on joint positions and velocities, and partial state output functions $y_i = h_i(\boldsymbol{q}, \boldsymbol{\eta}(t))$ depending only on the joint positions.

Full state output function: These output functions $y_i = h_i(\boldsymbol{x}, \boldsymbol{\eta}(t))$ represent, for example, constraints on the velocity of the manipulator or combinations of joint velocity and position limits. If the velocity constraint is on joint level, the output function only depends on the joint velocities $\dot{\boldsymbol{q}}$, whereas if the constraint is on task space level, the output function may depend on the joint velocities $\dot{\boldsymbol{q}}$ as well as on

Published version in IEEE Transactions on Robotics
Vol. 33, Issue 6, Dec. 2017
DOI: 10.1109/TRO.2017.2750697

the joints $\boldsymbol{q}$ due to the transformation (5). Differentiation with respect to time and using the system equation (11) yields

$$\begin{aligned}\dot{y}_i &= \frac{\partial h_i}{\partial \dot{\boldsymbol{q}}}\ddot{\boldsymbol{q}} + \frac{\partial h_i}{\partial \boldsymbol{q}}\dot{\boldsymbol{q}} + \frac{\partial h_i}{\partial \boldsymbol{\eta}}\dot{\boldsymbol{\eta}} \\ &= \frac{\partial h_i}{\partial \dot{\boldsymbol{q}}}\boldsymbol{M_q}^{-1}\boldsymbol{\tau}_\mathrm{c} - \frac{\partial h_i}{\partial \dot{\boldsymbol{q}}}\boldsymbol{M_q}^{-1}\left(\boldsymbol{C_q}\dot{\boldsymbol{q}} + \boldsymbol{g_q} + \boldsymbol{e}_\tau\right) \\ &\quad + \frac{\partial h_i}{\partial \boldsymbol{q}}\dot{\boldsymbol{q}} + \frac{\partial h_i}{\partial \boldsymbol{\eta}}\dot{\boldsymbol{\eta}} \ .\end{aligned}$$

Based on the derivative, the pseudo input z_i of the linearized system is determined by (12) with

$$\boldsymbol{a}_i^\mathsf{T}(\boldsymbol{x}, \boldsymbol{\eta}(t)) = \frac{\partial h_i}{\partial \dot{\boldsymbol{q}}}\boldsymbol{M_q}^{-1} \tag{14}$$

$$\begin{aligned}b_i(\boldsymbol{x}, \boldsymbol{\eta}(t), \ldots, \boldsymbol{\eta}^{(r_i)}(t)) &= -\frac{\partial h_i}{\partial \dot{\boldsymbol{q}}}\boldsymbol{M_q}^{-1}\left(\boldsymbol{C_q}\dot{\boldsymbol{q}} + \boldsymbol{g_q} + \boldsymbol{e}_\tau\right) \\ &\quad + \frac{\partial h_i}{\partial \boldsymbol{q}}\dot{\boldsymbol{q}} + \frac{\partial h_i}{\partial \boldsymbol{\eta}}\dot{\boldsymbol{\eta}}\end{aligned} \tag{15}$$

The system input $\boldsymbol{\tau}_\mathrm{c}$ appears already in the first time-derivative of the output and therefore $r_i = 1$ holds. For the relative degree to be well-defined, Assumption 5 has to hold. Similarly, the pseudo input corresponding to partial state output functions is derived.

Partial state output function: Output functions $y_i = h_i(\boldsymbol{q}, \boldsymbol{\eta}(t))$ may represent, for example, static joint limits or obstacles/bounds in task space. As task space limits may be transformed into joint space using (4), the functions depend solely on the joints $\boldsymbol{q}$ and differentiation with respect to time yields

$$\begin{aligned}\dot{y}_i &= \frac{\partial h_i}{\partial \boldsymbol{q}}\dot{\boldsymbol{q}} + \frac{\partial h_i}{\partial \boldsymbol{\eta}}\dot{\boldsymbol{\eta}} \ , \\ \ddot{y}_i &= \frac{\partial \dot{y}_i}{\partial \dot{\boldsymbol{q}}}\ddot{\boldsymbol{q}} + \frac{\partial \dot{y}_i}{\partial \boldsymbol{q}}\dot{\boldsymbol{q}} + \frac{\partial \dot{y}_i}{\partial \boldsymbol{\eta}}\dot{\boldsymbol{\eta}} + \frac{\partial \dot{y}_i}{\partial \dot{\boldsymbol{\eta}}}\ddot{\boldsymbol{\eta}} \\ &= \frac{\partial h_i}{\partial \boldsymbol{q}}\boldsymbol{M_q}^{-1}\boldsymbol{\tau}_\mathrm{c} - \frac{\partial h_i}{\partial \boldsymbol{q}}\boldsymbol{M_q}^{-1}\left(\boldsymbol{C_q}\dot{\boldsymbol{q}} + \boldsymbol{g_q} + \boldsymbol{e}_\tau\right) \\ &\quad + \frac{\partial}{\partial \boldsymbol{q}}\left(\frac{\partial h_i}{\partial \boldsymbol{q}}\dot{\boldsymbol{q}}\right)\dot{\boldsymbol{q}} + 2\frac{\partial}{\partial \boldsymbol{\eta}}\left(\frac{\partial h_i}{\partial \boldsymbol{q}}\dot{\boldsymbol{q}}\right)\dot{\boldsymbol{\eta}} \\ &\quad + \frac{\partial}{\partial \boldsymbol{\eta}}\left(\frac{\partial h_i}{\partial \boldsymbol{\eta}}\dot{\boldsymbol{\eta}}\right)\dot{\boldsymbol{\eta}} + \frac{\partial h_i}{\partial \boldsymbol{\eta}}\ddot{\boldsymbol{\eta}} \ .\end{aligned}$$

Again, the pseudo input z_i of the linearized system is determined by (12), in this case with

$$\boldsymbol{a}_i^\mathsf{T}(\boldsymbol{x}, \boldsymbol{\eta}(t)) = \frac{\partial h_i}{\partial \boldsymbol{q}}\boldsymbol{M_q}^{-1} \ , \tag{16}$$

$$\begin{aligned}b_i(\boldsymbol{x}, \boldsymbol{\eta}(t), \ldots, \boldsymbol{\eta}^{(r_i)}(t)) &= -\frac{\partial h_i}{\partial \boldsymbol{q}}\boldsymbol{M_q}^{-1}\left(\boldsymbol{C_q}\dot{\boldsymbol{q}} + \boldsymbol{g_q} + \boldsymbol{e}_\tau\right) \\ &\quad + \frac{\partial}{\partial \boldsymbol{q}}\left(\frac{\partial h_i}{\partial \boldsymbol{q}}\dot{\boldsymbol{q}}\right)\dot{\boldsymbol{q}} + \frac{\partial h_i}{\partial \boldsymbol{\eta}}\ddot{\boldsymbol{\eta}} + \frac{\partial}{\partial \boldsymbol{\eta}}\left(2\frac{\partial h_i}{\partial \boldsymbol{q}}\dot{\boldsymbol{q}} + \frac{\partial h_i}{\partial \boldsymbol{\eta}}\dot{\boldsymbol{\eta}}\right)\dot{\boldsymbol{\eta}} \ .\end{aligned} \tag{17}$$

The relative degree $r_i = 2$ is well-defined due to Assumption 5.

Although the output functions are defined in the generalized coordinates $\boldsymbol{q}$, task space constraints are also enforced. Using the forward kinematics (4) of the robotic system and the corresponding velocity transformation (5), it is possible to express task space constraints in the generalized coordinates and the I/O-linearization and the relative degree are determined by either (14)–(15) or (16)–(17).

B. Invariance functions and invariant set

The necessity of a switch to a corrective control input is determined by the so-called invariance function. This invariance function depends on the output function as well as the dynamics of the system and the relative degree. Neglecting the internal dynamics, the I/O-linearized system is represented by a time-invariant integrator chain [36]. Since $z_i(t)$ is the input of the integrator chain, it determines the behavior of the output $h_i(\boldsymbol{x}, \boldsymbol{\eta}(t))$. The goal of the control scheme is to keep the system within the admissible set (10), i.e. to keep the value of the output function at a non-positive value. For a negative input $z_i(t) < 0$ of the integrator chain, a reduction of the output is eventually achieved. This motivates the invariance control approach. The pseudo input is set to a constant, non-positive value $z_i(t) = \gamma_i \leq 0$ at time t when the value $z_i(t) = \gamma_i$ just suffices to keep the system within the admissible set. In order to find that instant of time, the dynamics of the integrator chain are investigated. In the following, we assume, that at time t, the system is within the admissible set, i.e. $h_i(\boldsymbol{x}, \boldsymbol{\eta}(t)) \leq 0$.

First, we consider a state output function, i.e. a system with $r_i = 1$. The integrator chain has only one state and the value of the output function at the future time t_f depending on the input $z_i(t) = \gamma_i$ and the current function value $h_i(\boldsymbol{x}, \boldsymbol{\eta}(t))$ is given by

$$\begin{aligned}h_i(\boldsymbol{x}, \boldsymbol{\eta}(t_f)) &= h_i(\boldsymbol{x}, \boldsymbol{\eta}(t)) + \int_t^{t_f} z_i(\zeta)d\zeta \\ &= h_i(\boldsymbol{x}, \boldsymbol{\eta}(t)) + (t_f - t)\gamma_i \ .\end{aligned}$$

Adherence to the limits is achieved, if $h_i(\boldsymbol{x}, \boldsymbol{\eta}(t_f)) \leq 0$ holds for all $t_f > t$. By deriving the function with respect to the future times

$$\frac{dh_i(\boldsymbol{x}, \boldsymbol{\eta}(t_f))}{dt_f} = \frac{d}{dt_f}(h_i(\boldsymbol{x}, \boldsymbol{\eta}(t)) + (t_f - t)\gamma_i) = \gamma_i \ , \tag{18}$$

it may be observed that the function is constant for $\gamma_i = 0$ and decreasing for $\gamma_i < 0$. As a result, the current value $h_i(\boldsymbol{x}, \boldsymbol{\eta}(t))$ is the maximum value the function will ever take for $\gamma_i \leq 0$ and applying $\gamma_i = 0$ at the instant of time, when $h_i(\boldsymbol{x}, \boldsymbol{\eta}(t)) = 0$ holds, avoids a violation of the constraint.

For a partial state output function, the integrator chain has two states and the future function values are determined by

$$\begin{aligned}h_i(\boldsymbol{x}, \boldsymbol{\eta}(t_f)) &= h_i(\boldsymbol{x}, \boldsymbol{\eta}(t)) + \int_t^{t_f}\left(\dot{h}_i(\boldsymbol{x}, \boldsymbol{\eta}(t)) + \int_t^{\vartheta} z_i(\zeta)d\zeta\right)d\vartheta \\ &= h_i(\boldsymbol{x}, \boldsymbol{\eta}(t)) + (t_f - t)\dot{h}_i(\boldsymbol{x}, \boldsymbol{\eta}(t)) + \frac{1}{2}(t_f - t)^2\gamma_i \ .\end{aligned}$$

The derivation with respect to t_f

$$\frac{dh_i(\boldsymbol{x}, \boldsymbol{\eta}(t_f))}{dt_f} = \dot{h}_i(\boldsymbol{x}, \boldsymbol{\eta}(t)) + (t_f - t)\gamma_i \tag{19}$$

shows that $h_i(\boldsymbol{x}, \boldsymbol{\eta}(t_f))$ is decreasing for $\dot{h}_i(\boldsymbol{x}, \boldsymbol{\eta}(t)) \leq 0$ and $\gamma_i < 0$ and therefore, the current value is the maximum of all future values. For $\dot{h}_i(\boldsymbol{x}, \boldsymbol{\eta}(t)) > 0$, however, the function takes its maximum at

$$t_f = t - \frac{\dot{h}_i(\boldsymbol{x}, \boldsymbol{\eta}(t))}{\gamma_i} \ , \tag{20}$$

which is obtained by setting (19) equal to zero and solving it for t_f. As a result, the maximum value of the output function is given by

$$h_i\left(\boldsymbol{x}, \boldsymbol{\eta}\left(t - \frac{\dot{h}_i(\boldsymbol{x}, \boldsymbol{\eta}(t))}{\gamma_i}\right)\right) = h_i(\boldsymbol{x}, \boldsymbol{\eta}(t)) - \frac{1}{2\gamma_i}\dot{h}_i^2(\boldsymbol{x}, \boldsymbol{\eta}(t)) \ . \tag{21}$$

If $z_i(t) = \gamma_i < 0$ is applied at the instant of time, when the maximum value is equal to zero, no violation of the constraint occurs.

Based on these results, we now introduce the invariance function with an expression corresponding to [23], [24]. The invariance function determines the instant of time t, when corrective action, i.e. $z_i = \gamma_i$, has to be applied. It depends on the relative degree and the current state values of the integrator chain. The invariance function $\Phi_i(\boldsymbol{x}, \boldsymbol{\eta}, \dot{\boldsymbol{\eta}}, \gamma_i)$ is given by

$$r_i = 1 : \ \Phi_i(\boldsymbol{x}, \boldsymbol{\eta}, \gamma_i) = y_i \tag{22}$$

$$r_i = 2 : \ \Phi_i(\boldsymbol{x}, \boldsymbol{\eta}, \dot{\boldsymbol{\eta}}, \gamma_i) = \begin{cases} y_i - \dfrac{1}{2\gamma_i}\dot{y}_i^2 & \dot{y}_i > 0 \\ y_i & \dot{y}_i \leq 0 \end{cases} \tag{23}$$

Published version in IEEE Transactions on Robotics
Vol. 33, Issue 6, Dec. 2017
DOI: 10.1109/TRO.2017.2750697

with $y_i = h_i(\boldsymbol{x}, \boldsymbol{\eta}(t))$ and $\dot{y}_i = \dot{h}_i(\boldsymbol{x}, \boldsymbol{\eta}(t), \dot{\boldsymbol{\eta}}(t))$. Intuitively, the invariance function represents the maximum value the output y_i will ever take in the future, if a constant corrective pseudo input $\gamma_i < 0$ is applied to the linearized system at time t. For $r_i = 1$, this means that at the instant t, $\dot{y}_i$ becomes negative. This constantly decreases the value of y_i, i.e. the current value is the maximum output, thus motivating (22). For $r_i = 2$, if $\dot{y}_i$ is already negative, the negative input will further decrease $\dot{y}_i$, which in turn decreases y_i. This, again, means that the current value is the maximum output, motivating the second case of (23). For $\dot{y}_i > 0$, y_i increases in value until the negative input γ_i reduces $\dot{y}_i$ to a non-positive value. The second case of (23) defines the value of y_i at the instant when $\dot{y}_i$ reverses its sign. If the invariance function of an output function takes a positive value, the corresponding constraint will be violated in the future. Based on the invariance functions, the invariant set

$$\mathcal{G}(t, \boldsymbol{\gamma}) = \{\boldsymbol{x} \in \mathbb{R}^{2n_q} \,|\, \Phi_i(\boldsymbol{x}, \boldsymbol{\eta}, \dot{\boldsymbol{\eta}}, \gamma_i) \leq 0 \quad \forall\, 1 \leq i \leq l\} \,, \tag{24}$$

describes the set of states, for which no constraint is violated, i.e. $h_i(\boldsymbol{x}, \boldsymbol{\eta}(t)) \leq 0$ for all $1 \leq i \leq l$, and no constraint will be violated in the future for the pseudo input $z_i = \gamma_i$. That means that the invariant set (24) is a subset of the admissible set (10). Note that for a constraint with relative degree one, both sets (24) and (10) are equal as the invariance function is equal to the output function. For constraints with a higher relative degree, e.g. position constraints on torque-controlled manipulators, consider the following example.

Example 1. *Let the system be a double integrator $\ddot{y} = u$ with the states y, $\dot{y}$ and the input u, which is constrained to $y \leq 0$. I/O-linearization yields a relative degree $r = 2$ and the input transformation $u = z$. Fig. 3 depicts the constraint (blue dashed line) and the corresponding admissible output values (light blue bars). First, we consider $y > 0$, i.e. the right half-plane. Here, the constraint is violated due to the positive value of the output and corrective action is required, which is illustrated by the the states being within the inadmissible set (red). For $\dot{y} < 0$ and $y \leq 0$, i.e. the bottom left quadrant, the negative value of $\dot{y}$ causes the output y to decrease. This means that while the states remain within the bottom left quadrant, no violation of the constraint occurs, independently from the input. No corrective action is necessary and the entire quadrant belongs to the admissible set* (10) *as well as the invariant set* (24)*. For $\dot{y} \geq 0$ and $y \leq 0$, consider the example $\dot{y} > 0$ and $y = 0$, for which the positive derivative will increase the output value y independently from the input, thus causing an immediate violation. Similarly, there are more values of y, $\dot{y}$, for which no corrective action exists which keeps the state within the admissible set. This is illustrated by the fact that part of the upper left quadrant is not within the invariant set, whereas the remainder is. The invariance function (red dotted line) from* (23) *divides the two parts. These are the state values, for which the negative corrective pseudo input γ just suffices to reduce $\dot{y}$ to zero when the output reaches $y = 0$.*

The example and Fig. 3 illustrate, that for $r = 2$ the invariant set is a proper subset of the admissible set. Similar relations hold for higher relative degrees.

In order to avoid any violation of the constraints, the goal should be to keep the system states in the invariant set and to initiate corrective action as soon as $\Phi_i(\boldsymbol{x}, \boldsymbol{\eta}, \dot{\boldsymbol{\eta}}, \gamma_i)$ reaches a value of zero. In consequence, $\Phi_i(\boldsymbol{x}, \boldsymbol{\eta}, \dot{\boldsymbol{\eta}}, \gamma_i) = 0$ determines the instant of time, when a corrective action is required such that a violation of the constraint is avoided.

C. Corrective control

The goal of corrective control is to render the system (11) controlled positive invariant with respect to (24), i.e. once the invariant set is entered, it will not be left anytime in the future.

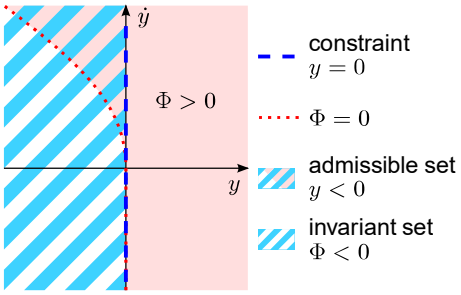

Fig. 3: Illustration of admissible and invariant set for $r = 2$.

Based on the previous considerations, we are now able to design a corrective pseudo input of the integrator chain. The input should enforce nominal behavior represented by

$$z_{\mathrm{no},i}(\boldsymbol{x}, \boldsymbol{\eta}, \dot{\boldsymbol{\eta}}, \ddot{\boldsymbol{\eta}}) = \boldsymbol{a}_i^{\mathsf{T}}(\boldsymbol{x}, \boldsymbol{\eta})\boldsymbol{\tau}_{\mathrm{no}} + b_i(\boldsymbol{x}, \boldsymbol{\eta}, \dot{\boldsymbol{\eta}}, \ddot{\boldsymbol{\eta}}) \tag{25}$$

in the I/O-linearized system (12), whenever possible. Additionally, it should enforce the required invariance with respect to (24). As determined in the previous section, corrective action is necessary for $\Phi_i(\boldsymbol{x}, \boldsymbol{\eta}, \dot{\boldsymbol{\eta}}, \gamma_i) \geq 0$. The corrective pseudo input is given by

$$r_i = 1 : z_{\mathrm{c},i}(t) = \begin{cases} \gamma_i & \text{if } t \in \mathcal{N}_{1a,i}(\gamma_i) \\ 0 & \text{if } t \in \mathcal{N}_{1b,i}(\gamma_i) \\ z_{\mathrm{no},i}(t) & \text{else.} \end{cases} \tag{26}$$

$$r_i = 2 : z_{\mathrm{c},i}(t) = \begin{cases} \gamma_i & \text{if } t \in (\mathcal{N}_{2a,i}(\gamma_i) \cup \mathcal{N}_{2b,i}(\gamma_i)) \\ 0 & \text{if } t \in (\mathcal{N}_{2c,i}(\gamma_i) \cup \mathcal{N}_{2d,i}(\gamma_i)) \\ z_{\mathrm{no},i}(t) & \text{else.} \end{cases} \tag{27}$$

with the sets

$$\mathcal{N}_{1a,i}(\gamma_i) = \{t | \Phi_i(\boldsymbol{x}(t), \boldsymbol{\eta}(t), \gamma_i) > 0\} \tag{28}$$
$$\mathcal{N}_{1b,i}(\gamma_i) = \{t | \Phi_i(\boldsymbol{x}(t), \boldsymbol{\eta}(t), \gamma_i) = 0\} \tag{29}$$
$$\mathcal{N}_{2a,i}(\gamma_i) = \{t | \Phi_i(\boldsymbol{x}(t), \boldsymbol{\eta}(t), \dot{\boldsymbol{\eta}}(t), \gamma_i) > 0 \wedge \dot{y}_i(t) \geq 0\} \tag{30}$$
$$\mathcal{N}_{2b,i}(\gamma_i) = \{t | \Phi_i(\boldsymbol{x}(t), \boldsymbol{\eta}(t), \dot{\boldsymbol{\eta}}(t), \gamma_i) = 0 \wedge \dot{y}_i(t) > 0\} \tag{31}$$
$$\mathcal{N}_{2c,i}(\gamma_i) = \{t | \Phi_i(\boldsymbol{x}(t), \boldsymbol{\eta}(t), \dot{\boldsymbol{\eta}}(t), \gamma_i) = 0 \wedge \dot{y}_i(t) = 0\} \tag{32}$$
$$\mathcal{N}_{2d,i}(\gamma_i) = \{t | \Phi_i(\boldsymbol{x}(t), \boldsymbol{\eta}(t), \dot{\boldsymbol{\eta}}(t), \gamma_i) > 0 \wedge \dot{y}_i(t) < 0\} \,. \tag{33}$$

With $\gamma_i < 0$, these pseudo control inputs achieve a system motion towards the invariant set for $\Phi_i(\boldsymbol{x}, \boldsymbol{\eta}, \dot{\boldsymbol{\eta}}, \gamma_i) > 0$.

Remark 4. *The magnitude of γ_i may be chosen arbitrarily. A large magnitude of γ_i reduces the time, during which corrective control is applied, since it is able to change the output value faster. As a result, it increases the size of the invariant set for for $r_i = 2$ defined by* (23) *and the magnitude of the required corrective control input. Equivalently, a small magnitude of γ_i increases the duration of corrective control use and decreases the size of the invariant set and the magnitude of the control input.*

Remark 5. *Due to the switching pseudo input, invariance controlled systems are prone to chattering in a sampled data implementation. This issue is addressed in [25].*

To control the robotic system, the pseudo input has to be transformed into a torque $\boldsymbol{\tau}_{\mathrm{c}}$. For this purpose, the set of active constraints

$$\mathcal{K}(t, \boldsymbol{\gamma}) = \{i \in \{1, 2, \ldots, l\} \,|\, \Phi_i(\boldsymbol{x}, \boldsymbol{\eta}, \dot{\boldsymbol{\eta}}, \gamma_i) \geq 0\} \tag{34}$$

is introduced, which determines the constraints requiring corrective action [24]. For the constraints, which are not in the active set, the application of nominal control suffices.

Published version in IEEE Transactions on Robotics
Vol. 33, Issue 6, Dec. 2017
DOI: 10.1109/TRO.2017.2750697

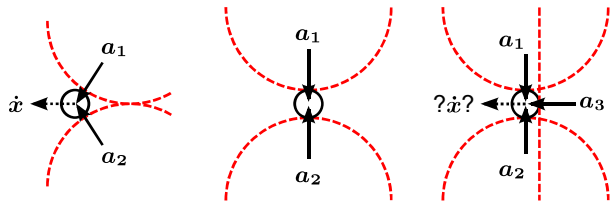

(a) (b) (c)

Fig. 4: Illustration of Assumption 6: In (a), an evasive motion $\dot{\boldsymbol{x}}$ may be derived as a linear combination of $\boldsymbol{a_1}, \boldsymbol{a_2}$, whereas in (b) this is not possible. In (c) an evasive motion is only defined if the constraint corresponding to $\boldsymbol{a_3}$ moves towards the state, otherwise the situation is similar to (b).

With the considerations on invariance in the previous section and the I/O-linearization (12), we receive an element-wise condition

$$\boldsymbol{z}_\mathcal{K} = \boldsymbol{A}_\mathcal{K}(\boldsymbol{x}, \boldsymbol{\eta}(t))\boldsymbol{\tau}_\mathrm{c} + \boldsymbol{b}_\mathcal{K}(\boldsymbol{x}, \boldsymbol{\eta}(t), \dot{\boldsymbol{\eta}}(t), \ddot{\boldsymbol{\eta}}(t)) \preccurlyeq \boldsymbol{z}_\mathrm{c} \ . \tag{35}$$

with $\boldsymbol{b}_\mathcal{K}(\boldsymbol{x}, \boldsymbol{\eta}(t), \dot{\boldsymbol{\eta}}(t), \ddot{\boldsymbol{\eta}}(t)) = [b_j(\boldsymbol{x}, \boldsymbol{\eta}(t), \dot{\boldsymbol{\eta}}(t), \ddot{\boldsymbol{\eta}}(t))]$, $\boldsymbol{z}_\mathcal{K} = [z_j]$ and $\boldsymbol{z}_\mathrm{c} = [z_{\mathrm{c},j}]$, the matrix $\boldsymbol{A}_\mathcal{K}(\boldsymbol{x}, \boldsymbol{\eta}) = [\boldsymbol{a}_j^\intercal(\boldsymbol{x}, \boldsymbol{\eta}(t))]$ and $j \in \mathcal{K}$. The entries of $\boldsymbol{b}_\mathcal{K}(\boldsymbol{x}, \boldsymbol{\eta}(t), \dot{\boldsymbol{\eta}}(t), \ddot{\boldsymbol{\eta}}(t))$ are calculated using the torque error $\boldsymbol{e}_\tau$, cf. (15) and (17), which is available from the underlying torque control loop. In order to improve readability, the explicit dependency on $\boldsymbol{x}$, $\boldsymbol{\eta}(t)$, $\dot{\boldsymbol{\eta}}(t)$ and $\ddot{\boldsymbol{\eta}}(t)$ is omitted for the matrix $\boldsymbol{A}(\boldsymbol{x}, \boldsymbol{\eta}(t))$, the vectors $\boldsymbol{a}_i^\intercal(\boldsymbol{x}, \boldsymbol{\eta}(t))$ and $\boldsymbol{b}(\boldsymbol{x}, \boldsymbol{\eta}(t), \dot{\boldsymbol{\eta}}(t), \ddot{\boldsymbol{\eta}}(t))$ and their respective elements in the following.

Solving the constrained minimization problem

$$\begin{aligned} &\underset{\boldsymbol{\tau}_\mathrm{c}}{\operatorname{argmin}} \|\boldsymbol{\tau}_\mathrm{c} - \boldsymbol{\tau}_\mathrm{no}\|_2^2 \\ &\text{s.t. (35)} \end{aligned} \tag{36}$$

yields corrective control. Due to the minimization, it is as close as possible to the nominal control input in the sense of the Euclidean distance. Using $\|\boldsymbol{\tau}\|_2^2 = \boldsymbol{\tau}^\intercal\boldsymbol{\tau}$ shows that (36) is equivalent to

$$\begin{aligned} &\underset{\boldsymbol{\tau}_\mathrm{c}}{\operatorname{argmin}} f(\boldsymbol{\tau}_\mathrm{c}, \boldsymbol{\tau}_\mathrm{no}) \\ &\text{s.t. (35)} \end{aligned} \tag{37}$$

with $f(\boldsymbol{\tau}_\mathrm{c}, \boldsymbol{\tau}_\mathrm{no}) = \boldsymbol{\tau}_\mathrm{c}^\intercal\boldsymbol{\tau}_\mathrm{c} - 2\boldsymbol{\tau}_\mathrm{c}^\intercal\boldsymbol{\tau}_\mathrm{no} + \boldsymbol{\tau}_\mathrm{no}^\intercal\boldsymbol{\tau}_\mathrm{no}$. The function $f(\boldsymbol{\tau}_\mathrm{c}, \boldsymbol{\tau}_\mathrm{no})$ is strictly convex in $\boldsymbol{\tau}_\mathrm{c}$, since its Hessian is the identity matrix $\boldsymbol{I}$, which is positive definite. Each of the inequality constraints (35) is linear and therefore convex. The set, over which the minimization is carried out is given by the intersection of the single constraints.

$$\mathcal{M} = \{\boldsymbol{\tau}_\mathrm{c} | \boldsymbol{A}_\mathcal{K}\boldsymbol{\tau}_\mathrm{c} + \boldsymbol{b}_\mathcal{K} - \boldsymbol{z}_{\mathcal{K},\mathrm{c}} \preccurlyeq 0\} \tag{38}$$

If no constraints are active, the set $\mathcal{M}$ contains all possible values of $\boldsymbol{\tau}_\mathrm{c}$. A solution to the minimization problem only exists, if the set (38) is non-empty, therefore, we make the following assumption.

Assumption 6. *The set $\mathcal{M}$, defined by the active constraints, is non-empty, $\mathcal{M} \neq \emptyset$.*

Figure 4 illustrates the meaning of Assumption 6. This assumption may seem a little restrictive, since obviously in Fig. 4b and 4c there exist admissible state trajectories. However, cases like in Fig. 4b and 4c rarely occur in reality. This would require an exact positioning of the limits with respect to the state such that the determined actions for the evasion two or more constraints exactly oppose one another.

By analyzing the characteristics of $\mathcal{M}$ more closely, it is possible to determine an analytic solution to the minimization (37). As the intersection of convex sets is, again, a convex set, $\mathcal{M}$ is convex. Therefore, the minimization problem (36) is strictly convex and any local minimum is the unique global minimum [37]. As a result, if $\boldsymbol{\tau}_\mathrm{no}$ is contained within the set, it is the only solution to the minimization. Otherwise, the minimum lies on the boundary of $\mathcal{M}$, i.e. some of the active constraints hold with equality

$$\mathcal{S}_\mathrm{eq} = \{i \in \mathcal{K} | \boldsymbol{a}_i^\intercal\boldsymbol{\tau}_\mathrm{c} + b_i = z_{\mathcal{K},\mathrm{c},i}\} \tag{39}$$

and some with strict inequality

$$\mathcal{S}_\mathrm{in} = \{i \in \mathcal{K} | \boldsymbol{a}_i^\intercal\boldsymbol{\tau}_\mathrm{c} + b_i < z_{\mathcal{K},\mathrm{c},i}\} = \mathcal{K} \setminus \mathcal{S}_\mathrm{eq} \ . \tag{40}$$

The equality constraints in $\mathcal{S}_\mathrm{eq}$ define a sub-manifold of the torque vector space. Not all of these constraints are necessarily required to define the sub-manifold. Instead, there exists a maximum subset of linearly independent constraints, which span the sub-manifold (39).

In the following, this maximum subset will be used to examine and illustrate the characteristics of the corrective control input determined by the solution of (36). Therefore, let the subset

$$\mathcal{I} = \{i \in \mathcal{S}_\mathrm{eq} \mid \operatorname{rank}(\boldsymbol{A}_\mathcal{I}) = |\mathcal{I}| \wedge \operatorname{rank}(\boldsymbol{A}_\mathcal{I}) = \operatorname{rank}(\boldsymbol{A}_{\mathcal{S}_\mathrm{eq}})\} \tag{41}$$

with $\boldsymbol{A}_\mathcal{I} = [\boldsymbol{a}_i^\intercal]$, $i \in \mathcal{I}$ and $\boldsymbol{A}_{\mathcal{S}_\mathrm{eq}} = [\boldsymbol{a}_i^\intercal]$, $i \in \mathcal{S}_\mathrm{eq}$, describe such a maximum subset of the constraints in $\mathcal{S}_\mathrm{eq}$ with linearly independent $\boldsymbol{a}_i^\intercal$. It is in general not uniquely defined, but any such set spans the sub-manifold $\mathcal{S}_\mathrm{eq}$. The remaining constraints $\mathcal{S}_\mathrm{eq} \setminus \mathcal{I}$ are determined by a linear combination of the constraints in $\mathcal{I}$. As the constraints in $\mathcal{I}$ span a subspace in the space of control torques and $\boldsymbol{\tau}_\mathrm{c} \in \mathbb{R}^{n_q}$, $|\mathcal{I}| \leq n_q$ holds. If $\mathcal{I}$ is empty, this means that either no constraints are active or all constraints hold with strict inequality, i.e. the nominal control signal is the minimum solution of (36). Assuming a set $\mathcal{I}$ has been determined, the solution to the minimization problem (36) is given by

$$\boldsymbol{\tau}_\mathrm{c} = \begin{cases} \boldsymbol{\tau}_\mathrm{no} & \text{if } \mathcal{I} = \emptyset \\ \boldsymbol{A}_\mathcal{I}^+(\boldsymbol{z}_{\mathcal{I},\mathrm{c}} - \boldsymbol{b}_\mathcal{I}) + (\boldsymbol{I} - \boldsymbol{A}_\mathcal{I}^+\boldsymbol{A}_\mathcal{I})\boldsymbol{\tau}_\mathrm{no} & \text{else} \end{cases} \tag{42}$$

with the Moore-Penrose pseudo inverse $\boldsymbol{A}_\mathcal{I}^+ = \boldsymbol{A}_\mathcal{I}^\intercal(\boldsymbol{A}_\mathcal{I}\boldsymbol{A}_\mathcal{I}^\intercal)^{-1}$. The matrix and vectors are determined by $\boldsymbol{A}_\mathcal{I} = [\boldsymbol{a}_i^\intercal]$, $\boldsymbol{b}_\mathcal{I} = [b_i]$ and $\boldsymbol{z}_{\mathcal{I},\mathrm{c}} = [z_{\mathrm{c},i}]$ with $i \in \mathcal{I}$. It remains to show whether the corrective control laws (36) and (42) actually render the robotic system (1) with input disturbances and time-varying boundary parameters invariant with respect to the invariant set (24).

IV. Control Properties

Although the theorems in the following are introduced for constraints of relative degree $r_i = \{1, 2\}$, they may be extended to higher relative degrees. Proofs are provided in the appendix.

A. Invariance

The goal of introducing invariance control is to guarantee adherence to constraints. As derived in the previous section, the invariant set (24) is a subset of the admissible set (10), which is determined by the constraints. Therefore, if the corrective input $\boldsymbol{\tau}_\mathrm{c}$ from (36) and (42) renders the system controlled positively invariant with respect to the invariant set, adherence to the constraints is guaranteed.

First, the invariance of the linearized system is investigated, i.e. the invariance of the integrator chains resulting from the I/O-linearization (12), which are controlled by the corrective pseudo inputs (26) and (27).

Lemma 1. *The integrator chain with r_i states, $r_i \in \{1, 2\}$, resulting from the I/O-linearization with respect to y_i* (12) *is rendered positively invariant with respect to the set* (24) *by any input $z_i \leq z_{c,i}$ with $z_{c,i}$ being the corresponding input from* (26) *and* (27).

Lemma 1 shows that the states of the linearized system remain within the invariant set. As control is applied to the nonlinear robotic

Published version in IEEE Transactions on Robotics
Vol. 33, Issue 6, Dec. 2017
DOI: 10.1109/TRO.2017.2750697

system (1), it is necessary to investigate whether the control torque, which is deduced from the linear analysis, provides the required invariance.

Theorem 1. *Let the robotic system be given by* (1) *and the outputs describing the constraints by* (9)*. Let the linearizing input be determined by* (12) *and the elements of the corrective pseudo input by* (26)–(27)*, depending on the relative degree. Let Assumptions 1, 3, 5 and 6 hold. Then, if the system states are within the invariant set at some time* $t = t_0$*, i.e.* $\boldsymbol{x}(t_0) \in \mathcal{G}(t_0, \boldsymbol{\gamma})$*, the corrective torque input determined by* (36) *will render the system controlled positively invariant with respect to the invariant set* (24) *for all* $t \geq t_0$*.*

Once the robotic system enters the invariant set, Theorem 1 guarantees that it stays within this set for all future times and therefore renders the system controlled positive invariant. Since the invariant set is a subset of the admissible set, the invariance control scheme ensures the adherence to the constraints. Note that the control law (42) achieves the same result, since it is the analytic solution of (36). As the system does not necessarily start in the invariant set, it remains to show that the system will eventually enter the invariant set.

Theorem 2. *Let the robotic system be given by* (1) *and the outputs describing the constraints by* (9)*. Let the linearizing input be determined by* (12) *and the elements of the corrective pseudo input by* (26)–(27)*, depending on the relative degree. Let Assumptions 1, 3, 5 and 6 hold. Then, if the system states lie outside of the invariant set at some instant of time* $t = t_0$*, i.e.* $\boldsymbol{x}(t_0) \notin \mathcal{G}(t_0, \boldsymbol{\gamma})$*, the corrective torque input determined by* (36) *guarantees that there exists a finite time interval* T *such that the system state enters and stays within the invariant set* (24) *for all* $t \geq t_0 + T$*.*

Theorem 2 shows that for invariance control, the initial state is not required to lie within the admissible set. Instead the control is such that after a finite time interval, the state becomes (and remains) admissible. By extension, this applies if additional constraints have to be included during runtime, e.g. when new obstacles appear.

Remark 6. *The results on the invariance of the controlled system are independent from nominal control. This means that whichever nominal control scheme is chosen, whether it is learned or explicitly defined, stable or unstable, the use in combination with invariance control results in adherence to the constraints.*

B. Boundedness

Naturally, good task performance of a robotic system under invariance control is only possible if constraint enforcement does not result in unboundedness of the tracking error. This is ensured by adding an additional constraint in the calculation of the corrective control input.

Theorem 3. *Let the robotic system be given by* (11) *and the outputs representing the constraints by* (9)*. Let a sufficiently smooth and bounded desired motion be given by* $\boldsymbol{x}_{des}(t)$ *and the initial state values within the invariant set* $\boldsymbol{x}(t_0) \in \mathcal{G}(t_0, \boldsymbol{\gamma})$*. Let further Assumptions 1–6 hold and let* $V(\boldsymbol{e})$ *be a Lyapunov function showing the global stability of the nominally controlled system. Then, if*

$$\mathcal{X} = \left\{ \boldsymbol{x} \,\middle|\, \exists\, t \geq t_0 \;:\; \operatorname{rank}\begin{bmatrix} \boldsymbol{A}_{\mathcal{K}}(\boldsymbol{x}, \boldsymbol{\eta}(t)) \\ \dfrac{\partial V(\boldsymbol{e})}{\partial \boldsymbol{e}} \boldsymbol{G}(\boldsymbol{x}) \end{bmatrix} = \operatorname{rank}(\boldsymbol{A}_{\mathcal{K}}(\boldsymbol{x}, \boldsymbol{\eta}(t))) \right\}$$

is bounded, there exist constants $\alpha, V_{\max} > 0$ *for which*

$$\begin{aligned} &\underset{\boldsymbol{\tau}_c}{\operatorname{argmin}} \|\boldsymbol{\tau}_c - \boldsymbol{\tau}_{no}\|_2^2 \qquad (43) \\ &\text{s.t. } \boldsymbol{A}_{\mathcal{K}}(\boldsymbol{x}, \boldsymbol{\eta}(t))\boldsymbol{\tau}_c + \boldsymbol{b}_{\mathcal{K}}(\boldsymbol{x}, \boldsymbol{\eta}(t), \dot{\boldsymbol{\eta}}(t), \ddot{\boldsymbol{\eta}}(t)) \preccurlyeq \boldsymbol{z}_{\mathcal{K},c} \\ &\quad \frac{\partial V(\boldsymbol{e})}{\partial \boldsymbol{e}}(\dot{\boldsymbol{x}}_{des} - \boldsymbol{f}(\boldsymbol{x}) - \boldsymbol{G}(\boldsymbol{x})\boldsymbol{\tau}_c) \leq B_{\dot{V}} \end{aligned}$$

$$\text{with } B_{\dot{V}} = \max(\alpha(V_{\max} - V(\boldsymbol{e})),\ \dot{V}_{no}(\boldsymbol{e}, \dot{\boldsymbol{e}}_{no}))\ ,$$
$$\dot{V}_{no}(\boldsymbol{e}, \dot{\boldsymbol{e}}_{no}) = \frac{\partial V(\boldsymbol{e})}{\partial \boldsymbol{e}}(\dot{\boldsymbol{x}}_{des} - \boldsymbol{f}(\boldsymbol{x}) - \boldsymbol{G}(\boldsymbol{x})\boldsymbol{\tau}_{no})$$

yields a uniquely defined corrective control input $\boldsymbol{\tau}_c$*, which renders the tracking error* $\boldsymbol{e} = \boldsymbol{x}_{des} - \boldsymbol{x}$ *at least bounded.*

In the following, we give a more intuitive understanding of Theorem 3, which provides an extended corrective control to bound the tracking error within the isoline $V(\boldsymbol{e}) = \max(V_{\max}, V(\boldsymbol{e}(t_0)))$.

Remark 7. *The goal of invariance control is to guarantee constraint enforcement also in cases when the desired trajectory leaves the admissible set, which is only possible if the tracking error is allowed to increase for such cases. Therefore it is natural that only boundedness of the tracking error is achieved.*

Remark 8. *Even if the initial state is not within the invariant set, the error is eventually bounded within* $\max(V_{\max}, V(\boldsymbol{e}(t_{inv})))$*, where* t_{inv} *is the instant of time when the state enters the admissible set, with* $t_{inv} < \infty$ *by Theorem 2.*

Remark 9. *In general, it is not trivial to determine whether the set* $\mathcal{X}$ *is bounded. If, however, the set of states itself only takes values from a bounded set* $\mathcal{X}_x \subset \mathbb{R}^{n_q}$*, i.e.* $\boldsymbol{x} \in \mathcal{X}_x$*, the set* $\mathcal{X}$ *is also bounded as* $\mathcal{X} \subseteq \mathcal{X}_x$ *holds. Since robotic systems are usually subject to joint and velocity limits, there the set of states is bounded thus fulfilling the requirement of Theorem 3.*

Bounding the tracking error while adhering to all constraints is only possible if the interior of $V(\boldsymbol{e}) = V_{\max}$ contains constraint admissible states for all instances of the desired trajectory and the constraint parameters. In order to determine such a $V_{\max}$, the behavior of the state on active constraints is examined. If there are active constraints, the derivative of the tracking error may be divided into a tangential and normal component with respect to these constraints. While the normal component is dictated by the constraint avoidance and possibly increases $\dot{V}$, the tangential component may be chosen freely to achieve $\dot{V} < 0$. If however, the state is in a local minimum of the Lyapunov function on the constraints, i.e. $V(\boldsymbol{e}) = V_{\min} = \min(V(\boldsymbol{e})|_{\boldsymbol{h}_{\mathcal{K}=\boldsymbol{0}}})$, further reduction of $\dot{V}$ via the tangential component is no longer possible. In that case the system needs to be able to follow the constraint motion for adherence by allowing a positive $\dot{V}$, which is achieved by choosing $V_{\max}$ such that $V_{\max} > \min(V(\boldsymbol{e})|_{\boldsymbol{h}_{\mathcal{K}=\boldsymbol{0}}})$ is fulfilled for all these minima and all possible combinations of active constraints and bounded parameters. The parameter α is then determined by the maximum increase in the Lyapunov function that is required for adherence in the local minima.

$$\alpha(V_{\max} - V_{\min})) > \max(\dot{V}|_{\boldsymbol{h}_{\mathcal{K}=\boldsymbol{0}}, V(\boldsymbol{e})=V_{\min}}) \qquad \forall\ V_{\min}$$

Remark 10. *If* $V_{\max}$ *and* α *are chosen too small, the optimization determining corrective control may be rendered infeasible. In view of the application, this issue is solved by increasing the values until a solution exists. However, on changing these values one needs to keep in mind that while* α *may be increased arbitrarily without deteriorating the task performance, an increase of* $V_{\max}$ *far beyond the minimally required value may lead to an increase in the bound on the tracking error.*

The following examples illustrate the implications of Theorem 3.

Example 2. *Consider the system of decoupled integrators* $\dot{\boldsymbol{x}} = \boldsymbol{u}$ *with* $\boldsymbol{x} = [x_1,\ x_2]^\intercal$*,* $\boldsymbol{x}(t_0) = [11,\ -85]^\intercal$*,* $\boldsymbol{u} = [u_1,\ u_2]^\intercal$ *and the nominal control law* $\boldsymbol{u} = [-0.1x_1,\ x_1 - 0.1x_2]^\intercal$*. The control law globally asymptotically stabilizes the system in the origin, which*

Published version in IEEE Transactions on Robotics
Vol. 33, Issue 6, Dec. 2017
DOI: 10.1109/TRO.2017.2750697

is validated using the Lyapunov function $V(\boldsymbol{x}) = \boldsymbol{x}^\intercal \boldsymbol{P}\boldsymbol{x}$ *with the positive definite matrix*

$$\boldsymbol{P} = \begin{bmatrix} 51 & 5 \\ 5 & 1 \end{bmatrix} .$$

The system is constrained by the output function $h(\boldsymbol{x}, t) = 9+\eta-x_1$ *with the bounded parameter* $\eta = \cos(2\pi t)$. *Derivation yields* $r = 1$ *and* $z = \dot{\eta} + [-1,\ 0]\boldsymbol{u}$. *As the Lyapunov function*

$$V(\boldsymbol{x}) = 51x_1^2 + 10x_1x_2 + x_2^2$$

and the constraint are convex, there exists exactly one minimum on the constraint, which takes its maximum value for $x_1 = 9+\max(\eta)$.

$$V_{\min} = \min(V)|_{h=0} = V(\boldsymbol{x})|_{\frac{\partial V}{\partial x2}=0} = 26x_1^2$$
$$\max(V_{\min}) = \min(V)|_{h=0,x_1=10} = 2600$$

By choosing $V_{\max} > 2600$, *it is assured that the isoline* $V(\boldsymbol{x}) = V_{\max}$ *always contains admissible states. If the state is in a minimum of the Lyapunov function on the constraint* $V_{\min}$, *the derivative*

$$\dot{V} = \begin{bmatrix} 102x_1 + 10x_2 & 10x_1 + 2x_2 \end{bmatrix} \begin{bmatrix} u_1 \\ u_2 \end{bmatrix}$$

maximally increases with the rate

$$\dot{V}|_{h=0,V_{\min}} = \begin{bmatrix} 52x_1 & 0 \end{bmatrix} \begin{bmatrix} \dot{\eta} \\ u_2 \end{bmatrix} = 52x_1\dot{\eta} \leq 52 \cdot 10 \cdot 2\pi \approx 3268$$

If $V_{\max}$ *and* α *are then chosen to fulfill*

$$\dot{V}|_{h=0,V_{\min}} \leq 3268 \leq \alpha(V_{\max} - \max(V_{\min})) ,$$

e.g. $V_{\max} = 2700$ *and* $\alpha = 35$, *the optimization from Theorem 3 is feasible and the solution renders the system bounded. Fig. 5a depicts the state trajectories of the unconstrained system behavior in comparison to the constrained system controlled with corrective control from* (36) *and Theorem 3. It is observed that while the unconstrained system approaches the origin asymptotically, both constrained trajectories remain at state values with* $x_1 > 8$ *due to the added constraint and the achieved invariance. The oscillation in the trajectories is due to the dynamic constraint. However, the state trajectory of the system controlled by* (36) *exhibits a growth in* x_2, *while the trajectory with control from Theorem 3 eventually ends up in a bounded limit cycle close to* $V(\boldsymbol{x}) = V_{\max}$.

Example 3. *Consider the same system and constraint as in the previous example but with nominal control* $\boldsymbol{u} = [-0.1x_1,\ -0.1x_2]^\intercal$. *The nominally controlled system is again globally asymptotically stable, which is shown by the Lyapunov function* $V(\boldsymbol{x}) = \boldsymbol{x}^\intercal\boldsymbol{x}$. *The same values of* $V_{\max}$ *and* α *as in the previous example are used. Fig. 5b depicts the state trajectories of the unconstrained system behavior in comparison to the constrained system controlled with corrective control from* (36) *and Theorem 3. Consistent with the previous example, the unconstrained system approaches the origin asymptotically but both constrained trajectories remain at state values with* $x_1 > 8$. *Here however, the state trajectories of both constrained systems are equivalent and are both bounded. This is due to the fact that in this case, the projection of nominal control onto the constraint results in a behavior that does not increase the Lyapunov function thus automatically fulfilling the additional condition of Theorem 3.*

V. Experimental Evaluation

In order to illustrate the capabilities of invariance control, an experiment is designed and conducted. The end effector of an anthropomorphic manipulator with 7 degrees of freedom ($n_q = 7$) is in direct contact with a human. One human exerts forces in order to achieve a desired behavior of the end effector. The manipulator reacts compliantly to those forces. A second human is moving in the vicinity of the robot. In order to keep this human safe, the robot should keep a safe distance at all times.

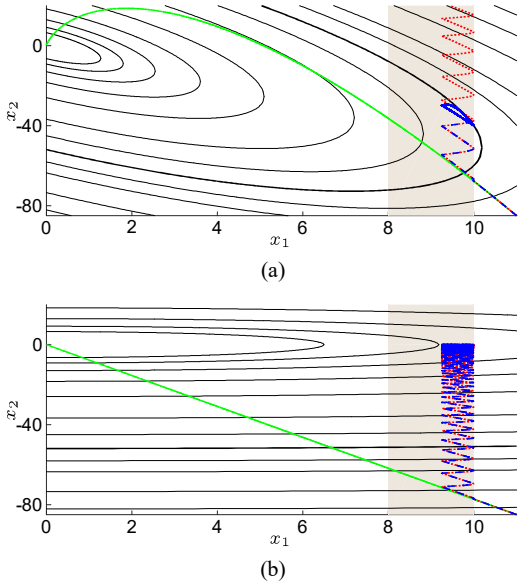

Fig. 5: State trajectories of (a) Example 2 and (b) Example 3 for ——— sole application of nominal control, ····· corrective control from (36) and - - - corrective control according to Theorem 3. The constraint moves within the shaded area and —— are the isolines of the Lyapunov function, where ——— represents $V(\boldsymbol{x}) = V_{\max}$.

Especially the application of the previously unknown, external disturbance forces illustrates the advantage of invariance control over collision avoidance approaches such as potential fields [18]. Even without knowledge of the magnitude or the direction of the applied force, invariance control is able to guarantee adherence to constraints, whereas potential functions are only able to give such a guarantee if they are designed to absorb all energy from the dynamics and the external forces, which would require prior knowledge.

A. Nominal control

The nominal control scheme is impedance control, which achieves the desired compliant behavior of the manipulator. Using task space impedance control (7) enables the design of the robot compliance in task space. A sensible choice of the parameters achieves the desired behavior in reaction to forces exerted by the human partner. The impedance control scheme does, however, not enforce the constraints.

B. Constraints

Constraints as in (9) are conveniently defined in Cartesian space, thus limiting the translational motion of the end effector. In the task at hand, the task space is the translational Cartesian space with the task coordinates $\boldsymbol{p}(t) \in \mathbb{R}^3$. The forward kinematics (4) and the Jacobian (5)–(6) are determined by the structure of the manipulator [38]. Typical shapes, which are used to model obstacles, are box or spherical constraints. Here, we choose one exemplary constraint to keep the human hand safe. Naturally, more constraints may be added to account for the entire human body.

Published version in IEEE Transactions on Robotics
Vol. 33, Issue 6, Dec. 2017
DOI: 10.1109/TRO.2017.2750697

We choose a spherical constraint with a fixed radius. In order to account for the moving human, the center position of the sphere varies over time. The output function is given by

$$y = h\left(\boldsymbol{p}(t), \begin{bmatrix} \boldsymbol{c_m}(t) \\ c_r \end{bmatrix}\right) = c_r - \|\boldsymbol{p}(t) - \boldsymbol{c_m}(t)\|_2 \ . \tag{44}$$

with the dynamic center position $\boldsymbol{c_m}(t) \in \mathbb{R}^3$ and the constant radius $c_r \in \mathbb{R}$. The parameters have to be chosen such that the human (or object) that has to be kept safe is contained entirely. Note that the radius and shape of the constraint may even be chosen to account for uncertainties in the motion.

C. Corrective Control

Based on the chosen constraint, corrective control is derived according to Sec. III. In the following, the explicit dependencies of the quantities are omitted for notational convenience, e.g. $\boldsymbol{p}(\boldsymbol{q}) = \boldsymbol{p}$, $\boldsymbol{a}^\intercal(\boldsymbol{p}, \boldsymbol{q}, \boldsymbol{c_m}) = \boldsymbol{a}^\intercal$. The I/O-linearization is determined by differentiating (44) with respect to time

$$\dot{y} = -\frac{(\boldsymbol{p} - \boldsymbol{c_m})^\intercal(\dot{\boldsymbol{p}} - \dot{\boldsymbol{c}}_{\boldsymbol{m}})}{\|\boldsymbol{p} - \boldsymbol{c_m}\|_2}$$
$$\ddot{y} = -\frac{(\boldsymbol{p}-\boldsymbol{c_m})^\intercal(\ddot{\boldsymbol{p}}-\ddot{\boldsymbol{c}}_{\boldsymbol{m}})+\|\dot{\boldsymbol{p}}-\dot{\boldsymbol{c}}_{\boldsymbol{m}}\|_2^2}{\|\boldsymbol{p}-\boldsymbol{c_m}\|_2} + \frac{((\boldsymbol{p}-\boldsymbol{c_m})^\intercal(\dot{\boldsymbol{p}}-\dot{\boldsymbol{c}}_{\boldsymbol{m}}))^2}{\|\boldsymbol{p}-\boldsymbol{c_m}\|_2^3} \ .$$

Using (5), differentiation yields

$$\ddot{\boldsymbol{p}} = \dot{\boldsymbol{J}}\dot{\boldsymbol{q}} + \boldsymbol{J}\ddot{\boldsymbol{q}} = \dot{\boldsymbol{J}}\dot{\boldsymbol{q}} + \boldsymbol{J}{\boldsymbol{M_q}}^{-1}(\boldsymbol{\tau}_\mathrm{c} - (\boldsymbol{C_q}\dot{\boldsymbol{q}} + \boldsymbol{g_q} + \boldsymbol{e}_\tau)) \ . \tag{45}$$

Assuming that $\frac{(\boldsymbol{p}-\boldsymbol{c_m})^\intercal}{\|\boldsymbol{p}-\boldsymbol{c_m}\|_2}\boldsymbol{J}{\boldsymbol{M_q}}^{-1}$ is non-singular for all times, the relative degree is $r = 2$ and the pseudo input (25) is given by

$$z = \ddot{y} = \boldsymbol{a}^\intercal\boldsymbol{\tau}_\mathrm{c} + b \tag{46}$$
$$\boldsymbol{a}^\intercal = \frac{(\boldsymbol{p} - \boldsymbol{c_m})^\intercal}{\|\boldsymbol{p} - \boldsymbol{c_m}\|_2}\boldsymbol{J}{\boldsymbol{M_q}}^{-1}$$
$$b = -\frac{(\boldsymbol{p} - \boldsymbol{c_m})^\intercal(\dot{\boldsymbol{J}}\dot{\boldsymbol{q}} - \boldsymbol{J}{\boldsymbol{M_q}}^{-1}(\boldsymbol{C_q}\dot{\boldsymbol{q}} + \boldsymbol{g_q} + \boldsymbol{e}_\tau) - \ddot{\boldsymbol{c}}_{\boldsymbol{m}})}{\|\boldsymbol{p} - \boldsymbol{c_m}\|_2} + \frac{\|\dot{\boldsymbol{p}} - \dot{\boldsymbol{c}}_{\boldsymbol{m}}\|_2^2}{\|\boldsymbol{p} - \boldsymbol{c_m}\|_2} + \frac{((\boldsymbol{p} - \boldsymbol{c_m})^\intercal(\dot{\boldsymbol{p}} - \dot{\boldsymbol{c}}_{\boldsymbol{m}}))^2}{\|\boldsymbol{p} - \boldsymbol{c_m}\|_2^3} \ .$$

The value of $\boldsymbol{c_m}$ and its time derivatives up to the second order are derived from the data collected using the motion tracking system. The torque error $\boldsymbol{e}_\tau$ is assumed to equal zero, which is validated by the positive experimental results. Since only one constraint is defined, determining the set $\mathcal{I}$ (41) is trivial and (42) may be used to determine corrective control. Note that the additional condition for boundedness from Theorem 3 does not need to be enforced in the experimental evaluation. Similar to Example 3, the combination of the constraint with nominal stiffness control yields a naturally bounded system.

D. Setup

Figure 6 depicts the actual experimental setup and Fig. 7 gives a more detailed schematic view. In general, the goal of introducing a safety control scheme is to keep humans in the vicinity safe. This requires tracking of the human body parts, e.g. by a vision-based perception system. Here, for the sake of demonstration, we employ our *Qualisys Motion Tracking System* to track and avoid any collision with a human hand. Note that since the control law only depends on the motion measurements but not on any model of the human movements, the results for different human subjects resemble one another apart from different humans choosing different trajectories. Therefore, we only show the results generated with one human. The hand is marked with a rigid body, the centroid of which defines the center position $\boldsymbol{c_m}(t)$ of the spherical constraint (44). The constant

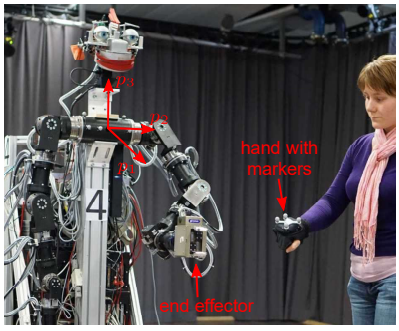

Fig. 6: The motion tracking system detects the markers on the hand. The centroid of the marker body defines the constraint center [29].

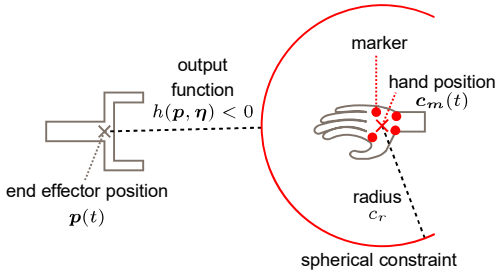

Fig. 7: The hand position determines the center $\boldsymbol{c_m}(t)$ of the spherical constraint with the constant radius c_r. The output function $h(\boldsymbol{p}, \boldsymbol{\eta})$ is a measure for the distance to the end effector [29].

radius c_r of the spherical constraint is then chosen such that the sphere encloses the human's hand.

The controlled robotic system is an anthropomorphic manipulator with seven degrees of freedom [38]. The joint position encoders measure the joint angles. Based on this measurement and the forward kinematics, the Cartesian position $\boldsymbol{p}(t)$ of the end effector is determined. The previously derived invariance control law, combining the nominal impedance control with the constraint, is implemented in the *Real-Time Workshop* of *Matlab/Simulink*, which uses a discrete-time Euler solver. The sampling frequency is 1 kHz. The external force $\boldsymbol{f}_\mathrm{ext} = \boldsymbol{J}(\boldsymbol{q})^\intercal\boldsymbol{\tau}_\mathrm{ext}$, applied to the end effector by the interacting human, is measured by a *JR3 sensor*, which senses forces and torques with 6 degrees of freedom.

The experiment is executed in two steps. During the entire time, the end effector tries to hold a desired nominal end effector position $\boldsymbol{p}_\mathrm{des}$ but reacts compliantly to exerted forces due to the nominal impedance control law. In a first trial, there is no physical contact between human and robot, i.e. no external forces, and the robot holds the desired position. The marked hand then approaches the end effector until an evading motion is carried out by the robot. In a second trial, a physical coupling between a human and the end effector is introduced, meaning that a second human firmly grasps the end effector and exerts forces to move the end effector in arbitrary directions. The nominal control and boundary parameters used in the experiment as well as the desired position of the end effector in robot base coordinates are provided in Table I.

E. Experimental evaluation

The experimental data is evaluated with respect to constraint adherence, i.e. invariance, and boundedness of the tracking error. The results obtained in the first step without external forces are

Published version in IEEE Transactions on Robotics
Vol. 33, Issue 6, Dec. 2017
DOI: 10.1109/TRO.2017.2750697

TABLE I: Experimental parameters

Cartesian stiffness	$\boldsymbol{K}_p$	$600\,\mathrm{N/m} \cdot \boldsymbol{I}_3$
Cartesian damping	$\boldsymbol{D}_p$	$80\,\mathrm{N\,s/m} \cdot \boldsymbol{I}_3$
Control parameter	γ	$-18\,\mathrm{m/s^2}$
Desired trajectory	$\boldsymbol{p}_{\mathrm{des}}$	$[0.635\ , 0.133\ , -0.441]^\intercal\,\mathrm{m}$
Constraint radius	c_r	$0.4\,\mathrm{m}$

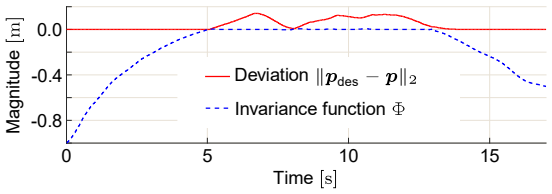

Fig. 8: Evaluation of the invariance function and the deviation from the desired position $\boldsymbol{p}_{\mathrm{des}}$ without external forces

illustrated in Fig. 8. The figure shows the value of the invariance function as well as the deviation of the end effector position from the desired position $\boldsymbol{p}_{\mathrm{des}}$. It may be observed that a bounded deviation from the desired position occurs when the invariance function is reduced to zero. Since the invariance function takes zero value when the system approaches the constraint, it is clear that a deviation has to occur in order to avoid a violation of the constraint. Apart from a slight chattering effect at zero, which results from the sampled time implementation of the continuous control scheme, the invariance function is never positive, which illustrates the invariance of the controlled system. A removal of the constraint, i.e. a motion of the human away from the end effector, allows the end effector to move back to the desired position.

Then, the physical contact with a human is established. Fig. 9a shows the fraction of the applied force, which is directed towards the constraint. The bounded deviation of the end effector from $\boldsymbol{p}_{\mathrm{des}}$ as shown in Fig. 9b is caused by the applied forces as well as by the approaching human hand. During the first $10\,\mathrm{s}$, the distance between the end effector (red line) and the constraint (green dash-dotted line)

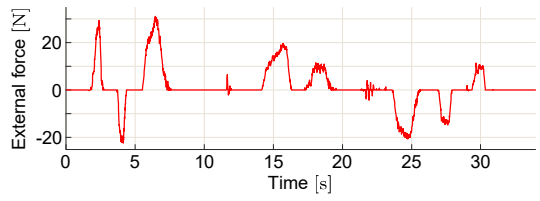

(a)

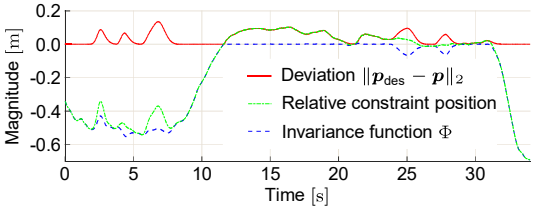

(b)

Fig. 9: Influence of (a) the magnitude of the applied external forces in direction of the constraint (positive for application in direction of the constraint) on (b) the deviation from the desired trajectory, the relative position of the constraint with respect to the end effector $\|\boldsymbol{p}_{\mathrm{des}} - \boldsymbol{p}\|_2 + y$ and the value of the invariance function

is large and the invariance function Φ is negative, i.e. the deviation is solely caused by the force. Naturally, the forces affect the value of Φ, since the output function (44) and Φ depend on the end effector position $\boldsymbol{p}(t)$. The figure shows that Φ only takes non-positive values, meaning that even in the presence of external forces, the robotic system is kept invariant by the control scheme and the constraint is not violated. For $\Phi = 0$, the system is at the boundary of the invariant set and the constraint is directly at the end effector, which is illustrated by the fact that the red and green lines coincide. The system reacts on the one hand compliantly to forces directed away from the constraint as for example at $t = 25\,\mathrm{s}$, which decrease the value of Φ and move the end effector away from the constraint. On the other hand, forces directed towards the constraint do not lead to a violation of the constraint or a positive value of Φ. Instead, the system is stiff and Φ keeps its value of zero as for example at $t = 15\,\mathrm{s}$. This emphasizes the fact, that invariance control renders a robotic system invariant and avoids constraint violation. Since the applied forces and the constraint motion are bounded, the deviation of the end effector from the desired position is also bounded throughout the experiment.

These results from the experiment encourage the application of invariance control to robotic systems in scenarios involving humans and physical interaction with humans.

VI. Conclusion

This article introduces a novel control scheme for robotic systems, which enables constraint admissible manipulation in dynamic environments as well as in close and physical interaction with humans. The derived control law is implemented in addition to a stabilizing nominal control law and only interferes with nominal behavior, to avoid the violation of a constraint, which allows the application in a variety of scenarios. Invariance control provides a method for defining an admissible set and determining a corrective control law, which keeps the system states in an invariant subset of the admissible set even in the presence of external forces and input disturbances. It renders the system positively invariant with respect to this set, thus guaranteeing constraint adherence. At the same time, the tracking error remains bounded. The provided experimental results illustrate the capabilities of the control scheme.

Acknowledgment

This work was supported by the EU Seventh Framework Programme FP7/2007-2013 within the ERC Starting Grant Control based on Human Models (con-humo), grant agreement no. 337654. The authors would like to thank the committed reviewers for their valuable comments.

Appendix A
Proofs

Proof of Lemma 1. The system is rendered invariant, if the invariance function describing the invariant set is not increasing at the boundary of the invariant set (24), where $\Phi_i(\boldsymbol{x}, \boldsymbol{\eta}, \dot{\boldsymbol{\eta}}, \gamma_i) = 0$ holds. We consider both relative degrees separately.

For $r_i = 1$, $\dot{y}_i = z_i \leq z_{\mathrm{c},i}$ holds and the invariance function is given by (22). For $\Phi_i(\boldsymbol{x}, \boldsymbol{\eta}, \gamma_i) = 0$, $z_{\mathrm{c},i} = 0$ is applied and

$$\dot{\Phi}_i(\boldsymbol{x}, \boldsymbol{\eta}, \gamma_i) = \dot{y}_i = z_i \leq z_{\mathrm{c},i} = 0\ ,$$
$$\frac{d^k}{dt^k}\Phi_i(\boldsymbol{x}, \boldsymbol{\eta}, \gamma_i) = 0 \quad \text{if } z_i = z_{\mathrm{c},i} = 0\ \forall k > 1$$

hold. The invariance function is not increasing on the boundary of the invariant set and the input renders the system invariant.

For $r_i = 2$, $\ddot{y}_i = z_i \leq z_{\mathrm{c},i}$ holds and the invariance function is given by (23). Again, $\Phi_i(\boldsymbol{x}, \boldsymbol{\eta}, \dot{\boldsymbol{\eta}}, \gamma_i) = 0$ holds on the boundary of

Published version in IEEE Transactions on Robotics
Vol. 33, Issue 6, Dec. 2017
DOI: 10.1109/TRO.2017.2750697

the invariant set, but now there are three cases to consider. For $\dot{y}_i > 0$, the pseudo input is given by $z_i \leq z_{\mathrm{c},i} = \gamma_i < 0$. For this input, the time derivative of the invariance function

$$\dot{\Phi}_i(\boldsymbol{x}, \boldsymbol{\eta}, \dot{\boldsymbol{\eta}}, \gamma_i) = \left(1 - \frac{1}{\gamma_i}\ddot{y}_i\right)\dot{y}_i \leq \left(1 + \frac{\gamma_i}{|\gamma_i|}\right)\dot{y}_i = 0$$

is negative for $z_i < z_{\mathrm{c},i} = \gamma_i < 0$ and equal to zero for $z_i = z_{\mathrm{c},i} = \gamma_i$. For $z_i = \gamma_i$, the higher order time derivatives are also equal to zero, since the constant factor carries through. Therefore, the invariance function is not increasing. For $\dot{y}_i < 0$, the time derivative of the invariance function is given by $\dot{\Phi}_i(\boldsymbol{x}, \boldsymbol{\eta}, \dot{\boldsymbol{\eta}}, \gamma_i) = \dot{y}_i < 0$. This means that the invariance function is decreasing independently from the control input. Finally, for $\dot{y}_i = 0$, the pseudo input is given by $z_i \leq z_{\mathrm{c},i} = 0$. The time derivatives of the invariance function

$$\begin{aligned}
\dot{\Phi}_i(\boldsymbol{x}, \boldsymbol{\eta}, \dot{\boldsymbol{\eta}}, \gamma_i) &= \dot{y}_i = 0 \\
\ddot{\Phi}_i(\boldsymbol{x}, \boldsymbol{\eta}, \dot{\boldsymbol{\eta}}, \gamma_i) &= \ddot{y}_i = z_i \leq z_{\mathrm{c},i} = 0 \\
\frac{d^k}{dt^k}\Phi_i(\boldsymbol{x}, \boldsymbol{\eta}, \dot{\boldsymbol{\eta}}, \gamma_i) &= 0 \quad \text{if } z_i = z_{\mathrm{c},i} = 0 \; \forall k > 2
\end{aligned}$$

show that the invariance function is not increasing. As a result, the control inputs (26) and (27) render an integrator chain with one and two states, respectively, invariant with respect to the set (24). □

Proof of Theorem 1. Corrective control is determined by the constrained minimization problem (36). The constraint, which has to be fulfilled by the control torque $\boldsymbol{\tau}_{\mathrm{c}}$, is given by (35). As a result from (12), the left side of the inequation is the pseudo input of the active constraints, generated by the control torque.

$$\boldsymbol{z}_{\mathcal{K}} = \boldsymbol{A}_{\mathcal{K}}\boldsymbol{\tau}_{\mathrm{c}} + \boldsymbol{b}_{\mathcal{K}} \tag{47}$$

Therefore, the input of the integrator chain resulting from the I/O-linearization fulfills the element-wise condition

$$\boldsymbol{z}_{\mathcal{K}} \preccurlyeq \boldsymbol{z}_{\mathcal{K},\mathrm{c}} \; . \tag{48}$$

An input $z_i \leq z_{\mathrm{c},i}$ for all active constraints renders an integrator chain invariant with respect to the invariant set, cf. Lemma 1. Additionally, the remaining inactive constraints are not in danger of violating a constraint and stay within the invariant set for any control action. Therefore, the solution of the constrained minimization problem provides a corrective control input, which renders the system controlled positive invariant with respect to the invariant set. □

Proof of Theorem 2. The system is outside of the invariant set, if at least one invariance function has a value larger than zero and it will enter the invariant set, if the control signal is such that the invariance functions result in non-positive values. Therefore, the system is guaranteed to enter the invariant set, if the control signal is such that any state trajectory starting outside of the invariant set is guaranteed to enter the set eventually.

For constraints with relative degree $r_i = 1$, the invariance function is given by (22). As the constraint is active, i.e. initially $y_{i,0} = y_i(t_0) > 0$, the input z_i of the linearized integrator chain fulfills $z_i = z_{\mathrm{c},i} \leq \gamma_i < 0$, cf. (26)–(36). As $\dot{y}_i = z_i$ holds for $r_i = 1$, $\dot{y}_i \leq \gamma_i < 0$ holds as long as the constraint is active, i.e. as long as y_i has a positive value. This means, that y_i and therefore also the value of the invariance function is decreasing until $y_i = 0$ is reached, when the system enters the invariant set of the constraint. Since $\dot{y}_i$ is strictly less than zero, this will happen in a finite time interval $T \leq \frac{y_{i,0}}{\gamma_i}$.

For constraints with relative degree $r_i = 2$, the integrator chain of the linearized system has two states y_i and $\dot{y}_i$. The invariance function is given by (23). The areas of the linearized state space, for which the invariance function has a positive value, are given by

(A) $\{\boldsymbol{x}, \boldsymbol{\eta} | y_i \leq 0 \wedge \dot{y}_i > 0 \wedge y_i > \frac{1}{2\gamma_i}\dot{y}_i^2\}$
(B) $\{\boldsymbol{x}, \boldsymbol{\eta} | y_i > 0 \wedge \dot{y}_i \geq 0\}$
(C) $\{\boldsymbol{x}, \boldsymbol{\eta} | y_i > 0 \wedge \dot{y}_i < 0\}$.

We now show that, starting from any arbitrary point in sets (A), (B) or (C), the system will eventually enter the invariant set.

First, assume the initial configuration lies within set (A). The constraint is active and $\ddot{y}_i = z_i \leq z_{\mathrm{c},i} = \gamma_i < 0$ holds, cf. (27)–(36). Since $\ddot{y}_i$ is strictly less than zero, $\dot{y}_i$ decreases and reaches zero after a finite time interval T_1. During that time, the output y_i increases its value since $\dot{y}_i > 0$ holds and may even become positive. If, after the time interval T_1, $y_i \leq 0$ holds, the system is within the invariant set, since $\dot{y}_i = 0$ holds. Otherwise, $y_i = 0$ and $\dot{y}_i > 0$ holds after a time interval $T < T_1$, meaning that the system enters the set (B).

Now assume, the initial configuration lies within (B). The constraint is active and $\ddot{y}_i = z_i \leq z_{\mathrm{c},i} = \gamma_i < 0$ holds, cf. (27)–(36). Similar to the previous case, $\dot{y}_i$ decreases and will reach a value of zero after a finite time interval T_2. During that time, the output y_i will further increase its value since $\dot{y}_i > 0$ holds. After the time interval T_2, $y_i > 0$ and $\dot{y}_i = 0$ holds, while the input is still strictly negative, meaning that the system enters set (C).

Finally, assume the initial configuration lies within (C). The constraint is active and $\ddot{y}_i = z_i \leq z_{\mathrm{c},i} = 0$, cf. (27)–(36). The value of y_i decreases, since $\dot{y}_i < 0$ within set (C). With $\ddot{y}_i \leq 0$, $\dot{y}_i$ either remains constant at its strictly negative value or decreases further. Therefore, after a finite time interval T_3, $y_i = 0$ is reached, while $\dot{y}_i < 0$ holds, meaning that the system enters the invariant set.

Therefore, for constraints with $r_i = 2$, starting from arbitrary states outside of the invariant set, the state trajectory evolves such that the invariant set is entered within a finite time interval $T_f \leq T_1 + T_2 + T_3$. The trajectory may either evolve from set (A) or (C) directly into the invariant set, from set (A) over sets (B) and (C) or from set (B) over set (C) into the invariant set. □

Proof of Theorem 3. This proof is conducted in two steps: First the existence of parameters $V_{\max}$ and α is shown, for which the optimization has a unique solution and second the resulting boundedness of the tracking error is proved.

In order to show that the minimization has a solution, it suffices to determine one input $\boldsymbol{\tau}_{\mathrm{c}}$ which fulfills both conditions: the invariance condition, which ensures constraint adherence, and the convergence condition, which guarantees boundedness. By Assumption 6, there exists a solution to (36), i.e. the minimization problem with solely the invariance condition. This solution is given by (42). The convergence condition on the other hand defines an upper bound on

$$\dot{V}(\boldsymbol{e}, \dot{\boldsymbol{e}}) = \frac{\partial V(\boldsymbol{e})}{\partial \boldsymbol{e}} \underbrace{(\dot{\boldsymbol{x}}_{\mathrm{des}} - \boldsymbol{f}(\boldsymbol{x}) - \boldsymbol{G}(\boldsymbol{x})\boldsymbol{\tau}_{\mathrm{c}})}_{\dot{\boldsymbol{e}}} \; .$$

For $\mathcal{I} = \emptyset$ with $\mathcal{I}$ from (41), the invariance condition has no influence on the solution and is fulfilled by $\boldsymbol{\tau}_{\mathrm{c}} = \boldsymbol{\tau}_{\mathrm{no}}$. In addition, $\boldsymbol{\tau}_{\mathrm{c}} = \boldsymbol{\tau}_{\mathrm{no}}$ also fulfills the convergence condition since then

$$\dot{V}(\boldsymbol{e}, \dot{\boldsymbol{e}}) = \dot{V}(\boldsymbol{e}, \dot{\boldsymbol{e}}_{\mathrm{no}}) \leq B_{\dot{V}}$$

with the bound $B_{\dot{V}}$ as defined in Theorem 3 holds for any value of $V_{\max}$ and α.

For $\mathcal{I} \neq \emptyset$, $\boldsymbol{\tau}_{\mathcal{I},\mathrm{c}} = \boldsymbol{A}_{\mathcal{I}}^{+}(\boldsymbol{z}_{\mathcal{I},\mathrm{c}} - \boldsymbol{b}_{\mathcal{I}}) + (\boldsymbol{I} - \boldsymbol{A}_{\mathcal{I}}^{+}\boldsymbol{A}_{\mathcal{I}})\boldsymbol{\tau}_{\mathrm{no}}$ from (42) solves the minimization (36) with only the invariance condition, i.e.

$$\boldsymbol{A}_{\mathcal{K}}\boldsymbol{\tau}_{\mathcal{I},\mathrm{c}} + \boldsymbol{b}_{\mathcal{K}} \leq \boldsymbol{z}_{\mathcal{K},\mathrm{c}}$$

holds. If by adding the convergence condition,

$$\operatorname{rank}\begin{bmatrix} \boldsymbol{A}_{\mathcal{K}} \\ \dfrac{\partial V(\boldsymbol{e})}{\partial \boldsymbol{e}}\boldsymbol{G}(\boldsymbol{x}) \end{bmatrix} > \operatorname{rank}(\boldsymbol{A}_{\mathcal{K}})$$

Published version in IEEE Transactions on Robotics
Vol. 33, Issue 6, Dec. 2017
DOI: 10.1109/TRO.2017.2750697

is fulfilled, then $\exists\ \boldsymbol{C}_\mathcal{K} \in \ker(\boldsymbol{A}_\mathcal{K}),\ \boldsymbol{C}_\mathcal{K} \notin \ker\left(\frac{\partial V(\boldsymbol{e})}{\partial \boldsymbol{e}}\boldsymbol{G}(\boldsymbol{x})\right)$. The input $\boldsymbol{\tau}_\mathrm{c} = \boldsymbol{\tau}_{\mathcal{I},\mathrm{c}} + \boldsymbol{C}_\mathcal{K}\boldsymbol{\tau}_{\mathcal{K},\mathrm{ker}}$ fulfills the invariance condition independently from $\boldsymbol{\tau}_{\mathcal{K},\mathrm{ker}}$ since

$$\begin{aligned}\boldsymbol{A}_\mathcal{K}\boldsymbol{\tau}_\mathrm{c} + \boldsymbol{b}_\mathcal{K} &= \boldsymbol{A}_\mathcal{K}(\boldsymbol{\tau}_{\mathcal{I},\mathrm{c}} + \boldsymbol{C}_\mathcal{K}\boldsymbol{\tau}_{\mathcal{K},\mathrm{ker}}) + \boldsymbol{b}_\mathcal{K} \\ &= \boldsymbol{A}_\mathcal{K}\boldsymbol{\tau}_{\mathcal{I},\mathrm{c}} + \underbrace{\boldsymbol{A}_\mathcal{K}\boldsymbol{C}_\mathcal{K}}_{=\boldsymbol{0}}\boldsymbol{\tau}_{\mathcal{K},\mathrm{ker}} + \boldsymbol{b}_\mathcal{K} = \boldsymbol{A}_\mathcal{K}\boldsymbol{\tau}_{\mathcal{I},\mathrm{c}} + \boldsymbol{b}_\mathcal{K}\ .\end{aligned}$$

As $\frac{\partial V(\boldsymbol{e})}{\partial \boldsymbol{e}}\boldsymbol{G}(\boldsymbol{x})\boldsymbol{C}_\mathcal{K} \neq \boldsymbol{0}$, there exists a $\boldsymbol{\tau}_{\mathcal{K},\mathrm{ker}}$, such that

$$\frac{\partial V(\boldsymbol{e})}{\partial \boldsymbol{e}}(\dot{\boldsymbol{x}}_\mathrm{des} - \boldsymbol{f}(\boldsymbol{x}) - \boldsymbol{G}(\boldsymbol{x})(\underbrace{\boldsymbol{\tau}_{\mathcal{I},\mathrm{c}} + \boldsymbol{C}_\mathcal{K}\boldsymbol{\tau}_{\mathcal{K},\mathrm{ker}}}_{\boldsymbol{\tau}_\mathrm{c}})) \leq \alpha(V_\mathrm{max} - V(\boldsymbol{e}))$$

is fulfilled for any choice of V_max and α, i.e. the convergence condition holds with $\dot{V}(\boldsymbol{e}, \dot{\boldsymbol{e}}) \leq \alpha(V_\mathrm{max} - V(\boldsymbol{e})) \leq B_{\dot{V}}$. On the other hand, if

$$\mathrm{rank}\begin{bmatrix}\boldsymbol{A}_\mathcal{K} \\ \dfrac{\partial V(\boldsymbol{e})}{\partial \boldsymbol{e}}\boldsymbol{G}(\boldsymbol{x})\end{bmatrix} = \mathrm{rank}(\boldsymbol{A}_\mathcal{K})$$

holds, the input $\boldsymbol{\tau}_\mathrm{c} = \boldsymbol{\tau}_{\mathcal{I},\mathrm{c}}$ fulfills the invariance condition as discussed above, whereas the left hand side

$$\begin{aligned}&\frac{\partial V(\boldsymbol{e})}{\partial \boldsymbol{e}}(\dot{\boldsymbol{x}}_\mathrm{des} - \boldsymbol{f}(\boldsymbol{x}) - \boldsymbol{G}(\boldsymbol{x})\boldsymbol{\tau}_{\mathcal{I},\mathrm{c}}) \\ &\quad= \underbrace{\dot{V}_\mathrm{no}(\boldsymbol{e}, \dot{\boldsymbol{e}}_\mathrm{no})}_{\leq 0} - \frac{\partial V(\boldsymbol{e})}{\partial \boldsymbol{e}}\boldsymbol{G}(\boldsymbol{x})\boldsymbol{A}_\mathcal{I}^+(\boldsymbol{z}_{\mathcal{I},\mathrm{c}} - \boldsymbol{b}_\mathcal{I} - \boldsymbol{A}_\mathcal{I}\boldsymbol{\tau}_\mathrm{no}) \\ &\quad\leq \underbrace{\frac{\partial V(\boldsymbol{e})}{\partial \boldsymbol{e}}\boldsymbol{G}(\boldsymbol{x})\boldsymbol{A}_\mathcal{I}^+(\overbrace{\boldsymbol{A}_\mathcal{I}\boldsymbol{\tau}_\mathrm{no} + \boldsymbol{b}_\mathcal{I}}^{\boldsymbol{z}_{\mathcal{I},\mathrm{no}}} - \boldsymbol{z}_{\mathcal{I},\mathrm{c}})}_{:= LHS(\boldsymbol{x}, \boldsymbol{x}_\mathrm{des}, \boldsymbol{\eta}, \dot{\boldsymbol{\eta}}, \ddot{\boldsymbol{\eta}})}\ .\end{aligned}$$

and the right hand side of the convergence condition

$$B_{\dot{V}} \geq \underbrace{\alpha(V_\mathrm{max} - V(\boldsymbol{e}))}_{:= RHS(\boldsymbol{e})}$$

are bounded by functions $LHS(\boldsymbol{x}, \boldsymbol{x}_\mathrm{des}, \boldsymbol{\eta}, \dot{\boldsymbol{\eta}}, \ddot{\boldsymbol{\eta}})$ and $RHS(\boldsymbol{e})$. The output functions and derivatives are continuous by Assumption 3, including $\boldsymbol{A}_\mathcal{K}$, $\boldsymbol{A}_\mathcal{K}^+$ and $\boldsymbol{b}_\mathcal{K}$. Nominal control is continuous by Assumption 2 and $\boldsymbol{G}(\boldsymbol{x})$ and the Lyapunov function are continuous as well. Since $\boldsymbol{z}_{\mathcal{I},\mathrm{no}}$ is an additive and multiplicative concatenation of continuous functions, it is continuous. As the parameters $\boldsymbol{\eta}$ and their derivatives are bounded by Assumption 3 and the desired trajectory $\boldsymbol{x}_\mathrm{des}$ is also assumed to be bounded, $\boldsymbol{z}_{\mathcal{I},\mathrm{no}}$ and as a result $\boldsymbol{z}_{\mathcal{I},\mathrm{c}}$ from (26), (27) and the functions $LHS(\boldsymbol{x}, \boldsymbol{x}_\mathrm{des}, \boldsymbol{\eta}, \dot{\boldsymbol{\eta}}, \ddot{\boldsymbol{\eta}})$ and $RHS(\boldsymbol{e})$ are bounded on any bounded set of states $\boldsymbol{x}$. Therefore, if

$$\mathcal{X} = \left\{\boldsymbol{x}\ \middle|\ \exists\ t \geq t_0 : \mathrm{rank}\begin{bmatrix}\boldsymbol{A}_\mathcal{K}(\boldsymbol{x}, \boldsymbol{\eta}(t)) \\ \dfrac{\partial V(\boldsymbol{e})}{\partial \boldsymbol{e}}\boldsymbol{G}(\boldsymbol{x})\end{bmatrix} = \mathrm{rank}(\boldsymbol{A}_\mathcal{K}(\boldsymbol{x}, \boldsymbol{\eta}(t)))\right\}$$

is bounded, the input $\boldsymbol{\tau}_\mathrm{c} = \boldsymbol{\tau}_{\mathcal{I},\mathrm{c}}$ is only applied on this bounded set of states $\boldsymbol{x}$ and there exist bounds

$$\begin{aligned}B_{LHS} &= \sup_\mathcal{X}\left(LHS(\boldsymbol{x}, \boldsymbol{x}_\mathrm{des}, \boldsymbol{\eta}, \dot{\boldsymbol{\eta}}, \ddot{\boldsymbol{\eta}})\right) \\ B_{RHS} &= \inf_\mathcal{X}(RHS(\boldsymbol{e})) = \alpha(V_\mathrm{max} - \sup_\mathcal{X}(V(\boldsymbol{e})))\ .\end{aligned}$$

By choosing the parameters V_max and α such that they fulfill

$$\sup_\mathcal{X}\left(LHS(\boldsymbol{x}, \boldsymbol{x}_\mathrm{des}, \boldsymbol{\eta}, \dot{\boldsymbol{\eta}}, \ddot{\boldsymbol{\eta}})\right) \leq \alpha(V_\mathrm{max} - \sup_\mathcal{X}(V(\boldsymbol{e})))\ ,$$

the convergence condition for $\boldsymbol{\tau}_\mathrm{c} = \boldsymbol{\tau}_{\mathcal{I},\mathrm{c}}$ is met as well since

$$\begin{aligned}\dot{V}(\boldsymbol{e}, \dot{\boldsymbol{e}}) &= \frac{\partial V(\boldsymbol{e})}{\partial \boldsymbol{e}}(\dot{\boldsymbol{x}}_\mathrm{des} - \boldsymbol{f}(\boldsymbol{x}) - \boldsymbol{G}(\boldsymbol{x})\boldsymbol{\tau}_{\mathcal{I},\mathrm{c}}) \\ &\leq LHS(\boldsymbol{x}, \boldsymbol{x}_\mathrm{des}, \boldsymbol{\eta}, \dot{\boldsymbol{\eta}}, \ddot{\boldsymbol{\eta}}) \leq \sup_\mathcal{X}\left(LHS(\boldsymbol{x}, \boldsymbol{x}_\mathrm{des}, \boldsymbol{\eta}, \dot{\boldsymbol{\eta}}, \ddot{\boldsymbol{\eta}})\right) \\ &\leq \alpha(V_\mathrm{max} - \sup_\mathcal{X}(V(\boldsymbol{e}))) \leq \alpha(V_\mathrm{max} - V(\boldsymbol{e})) \leq B_{\dot{V}}\end{aligned}$$

holds for all $\boldsymbol{x} \in \mathcal{X}$. Hence in all cases, there exists at least one $\boldsymbol{\tau}_\mathrm{c}$, which solves the minimization problem but which is not necessarily the optimal solution. Since, however the optimization is strictly convex, there exists a unique solution to the problem.

With the existence of a corrective control input established, we turn to the tracking error. The solution of the minimization fulfills

$$\dot{V}(\boldsymbol{e}, \dot{\boldsymbol{e}}) \leq \max(\alpha(V_\mathrm{max} - V(\boldsymbol{e})),\ \dot{V}_\mathrm{no}(\boldsymbol{e}, \dot{\boldsymbol{e}}_\mathrm{no}))\ .$$

Additionally for $V(\boldsymbol{e}) > V_\mathrm{max}$, the right hand side is non-positive, as $\alpha(V_\mathrm{max} - V(\boldsymbol{e})) < 0$ holds and $\dot{V}_\mathrm{no}(\boldsymbol{e}, \dot{\boldsymbol{e}}_\mathrm{no}) \leq 0$ by Assumption 2. Therefore, $\dot{V}(\boldsymbol{e}, \dot{\boldsymbol{e}}) \leq 0$ holds, which means that the Lyapunov function is bounded with $V(\boldsymbol{e}) \leq \max(V_\mathrm{max}, V(\boldsymbol{e}(t_0)))$. As $V(\boldsymbol{e})$ is a Lyapunov function showing global stability of the tracking error, it is continuous and radially unbounded, meaning that if the norm of $\boldsymbol{e}$ goes to infinity, so will $V(\boldsymbol{e})$. Therefore by the converse argument, if $V(\boldsymbol{e})$ is bounded, so is $\boldsymbol{e}$. □

References

[1] J.L. Pons. Rehabilitation Exoskeletal Robotics. *IEEE Eng. Med. Biol. Mag.*, 29(3):57–63, 2010.

[2] J.R. Medina Hernández, M. Lawitzky, A. Mörtl, D. Lee, and S. Hirche. An Experience-Driven Robotic Assistant Acquiring Human Knowledge to Improve Haptic Cooperation. In *IEEE/RSJ Int. Conf. on Intelligent Robots and Systems (IROS)*, pages 2416–2422, 2011.

[3] A. Mörtl, M. Lawitzky, A. Kucukyilmaz, M. Sezgin, C. Basdogan, and S. Hirche. The Role of Roles: Physical Cooperation between Humans and Robots. *The Int. Journal of Robotics Research (IJRR)*, 31(13):1656–1674, 2012.

[4] ISO. Robots and robotic devices – Safety requirements for personal care robots. ISO 13482:2014, International Organization for Standardization, Geneva, Switzerland, 2014.

[5] ISO. Robots and robotic devices – Collaborative robots. ISO 15066:2016, International Organization for Standardization, Geneva, Switzerland, 2016.

[6] R.M. Murray, Z. Li, and S.S. Sastry. *A Mathematical Introduction to Robotic Manipulation*. CRC Press, 1994.

[7] A. Albu-Schäffer, C. Ott, U. Frese, and G. Hirzinger. Cartesian Impedance Control of Redundant Robots: Recent Results with the DLR-Light-Weight-Arms. In *IEEE Int. Conf. on Robotics and Automation (ICRA)*, volume 3, pages 3704–3709, Sept. 2003.

[8] S.D. Whitehead, R.S. Sutton, and D.H. Ballard. Advances in Reinforcement Learning and Their Implications for Intelligent Control. In *5th IEEE Int. Symp. on Intelligent Control*, volume 2, pages 1289–1297, 1990.

[9] L. Buşoniu, R. Babuška, and B. De Schutter. Multi-Agent Reinforcement Learning: A Survey. In *9th Int. Conf. on Control, Automation, Robotics and Vision (ICARCV)*, pages 1–6, 2006.

[10] D.Q. Mayne, J.B. Rawlings, C.V. Rao, and P.O.M. Scokaert. Constrained model predictive control: Stability and optimality. *Automatica*, 36(6):789–814, 2000.

[11] E. Gilbert and I. Kolmanovsky. Nonlinear tracking control in the presence of state and control constraints: a generalized reference governor. *Automatica*, 38(12):2063–2073, 2002.

[12] D. Angeli and E. Mosca. Command Governors for Constrained Nonlinear Systems. *IEEE Trans. Autom. Control*, 44(4):816–820, 1999.

[13] A. Vahidi, I. Kolmanovsky, and A. Stefanopoulou. Constraint Handling in a Fuel Cell System: A Fast Reference Governor Approach. *IEEE Trans. Control Syst. Technol.*, 15(1):86–98, 2007.

[14] S. Prajna and A. Rantzer. Convex Programs for Temporal Verification of Nonlinear Dynamical Systems. *SIAM Journal on Control and Optimization*, 46(3):999–1021, 2007.

Published version in IEEE Transactions on Robotics
Vol. 33, Issue 6, Dec. 2017
DOI: 10.1109/TRO.2017.2750697

[15] A.D. Ames, J.W. Grizzle, and P. Tabuada. Control Barrier Function based Quadratic Programs with Application to Adaptive Cruise Control. In *IEEE 53rd Annu. Conf. on Decision and Control (CDC)*, pages 6271–6278, 2014.
[16] M. Rauscher, M. Kimmel, and S. Hirche. Constrained Robot Control Using Control Barrier Functions. In *IEEE/RSJ Int. Conf. on Intelligent Robots and Systems (IROS)*, pages 279–285, Daejeon, Korea, 2016.
[17] J. Jiang and A. Astolfi. Shared-Control for the Kinematic Model of a Mobile Robot. In *IEEE 53rd Annu. Conf. on Decision and Control (CDC)*, pages 62–67, 2014.
[18] E. Rimon and D.E. Koditschek. Exact Robot Navigation Using Artificial Potential Functions. *IEEE Trans. Robot. Autom.*, 8(5):501–518, 1992.
[19] D. Fox, W. Burgard, and S. Thrun. The Dynamic Window Approach to Collision Avoidance. *IEEE Robot. Autom. Mag.*, 4(1):23–33, 1997.
[20] B. Gillespie and M. Cutkosky. Stable User-Specific Haptic Rendering of the Virtual Wall. In *ASME Int. Mechanical Engineering Congr. & Expo.*, volume 58, pages 397–406, 1996.
[21] J. J. Abbott, P. Marayong, and A. M. Okamura. Haptic Virtual Fixtures for Robot-Assisted Manipulation. In R. Brooks S. Thrun and H. Durrant-Whyte, editors, *Robotics Research: Results of the 12th Int. Symp. ISRR (Springer Tracts in Advanced Robotics)*, volume 28, pages 49–64. Springer Berlin Heidelberg, Berlin, Heidelberg, 2007.
[22] J. Mareczek, M. Buss, and G. Schmidt. Sufficient Conditions for Invariance Control of a Class of Nonlinear Systems. In *IEEE 39th Annu. Conf. on Decision and Control (CDC)*, pages 1436–1442, Sydney, Australia, 2000.
[23] J. Wolff and M. Buss. Invariance Control Design for Nonlinear Control Affine Systems under Hard State Constraints. In *6th IFAC Symp. on Nonlinear Control Systems (NOLCOS)*, pages 711–716, Stuttgart, Germany, 2004.
[24] M. Scheint, J. Wolff, and M. Buss. Invariance Control in Robotic Applications: Trajectory Supervision and Haptic Rendering. In *American Control Conf. (ACC)*, pages 1436–1442, Seattle, USA, 2008.
[25] M. Kimmel and S. Hirche. Invariance Control with Chattering Reduction. In *IEEE 53rd Annu. Conf. on Decision and Control (CDC)*, pages 68–74, 2014.
[26] M. Sobotka, J. Wolff, and M. Buss. Invariance Controlled Balance of Legged Robots. In *European Control Conf. (ECC)*, pages 2–5, 2007.
[27] M. Kimmel, M. Lawitzky, and S. Hirche. 6D Workspace Constraints for Physical Human-Robot Interaction using Invariance Control with Chattering Reduction. In *IEEE/RSJ Int. Conf. on Intelligent Robots and Systems (IROS)*, pages 3377–3383, 2012.
[28] M. Kimmel and S. Hirche. Invariance Control with Time-varying Constraints. In *European Control Conf. (ECC)*, pages 867–872, 2016.
[29] M. Kimmel and S. Hirche. Active Safety Control for Dynamic Human-Robot Interaction. In *IEEE/RSJ Int. Conf. on Intelligent Robots and Systems (IROS)*, pages 4685–4691, Hamburg, Germany, 2015.
[30] A. Albu-Schäffer, O. Eiberger, M. Grebenstein, S. Haddadin, C. Ott, T. Wimböck, S. Wolf, and G. Hirzinger. Soft Robotics. *IEEE Robot. Autom. Mag.*, 15(3):20–30, Sept. 2008.
[31] C. Ott, A. Albu-Schäffer, A. Kugi, and G. Hirzinger. On the Passivity-Based Impedance Control of Flexible Joint Robots. *IEEE Trans. Robot.*, 24(2):416–429, 2008.
[32] A. Bicchi and G. Tonietti. Fast and "Soft-Arm" Tactics [Robot Arm Design]. *IEEE Robot. Autom. Mag.*, 11(2):22–33, 2004.
[33] A. De Santis, A. Albu-Schäffer, C. Ott, B. Siciliano, and G. Hirzinger. The skeleton algorithm for self-collision avoidance of a humanoid manipulator. In *IEEE/ASME Int. Conf. on Advanced Intelligent Mechatronics (AIM)*, pages 1–6, Sept. 2007.
[34] T. Flash and N. Hogan. The Coordination of Arm Movements: An Experimentally Confirmed Mathematical Model. *The Journal of Neuroscience*, 5(7):1688–1703, July 1985.
[35] K. Sekiguchi and M. Sampei. Change of controller based on partial feedback linearization with time-varying function. In *IEEE 51st Annu. Conf. on Decision and Control (CDC)*, pages 3557–3563, 2012.
[36] S. Palanki and C. Kravaris. Controller synthesis for time-varying systems by input/output linearization. *Computers & Chemical Engineering*, 21(8):891–903, 1997.
[37] S. P. Boyd. *Convex Optimization*. Cambridge University Press, 2004.
[38] B. Stanczyk and M. Buss. Development of a Telerobotic System for Exploration of Hazardous Environments. In *IEEE/RSJ Int. Conf. on Intelligent Robots and Systems (IROS)*, pages 2532–2537, 2004.

Melanie Kimmel received her M.Sc. degree in Electrical and Computer Engineering from the Technical University of Munich, Munich, Germany in 2013. Since November 2013 she is working towards a Doctor of Engineering degree in Electrical and Computer Engineering at the Chair of Information-oriented Control, Department of Electrical and Computer Engineering, Technical University of Munich (TUM), Germany. Her research interests include robot control for safe human-robot interaction and control under environmental uncertainties and constraints.

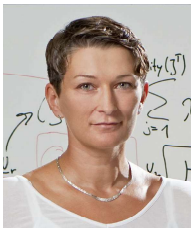

Sandra Hirche received the Diplom degree in Mechanical Engineering and Transport Systems from the Technical University Berlin, Germany, in 2002 and the Doctor of Engineering degree in Electrical Engineering and Information Technology from the Technical University of Munich, Munich, Germany, in 2005. From 2005 to 2007 she was awarded a Postdoc scholarship from the Japanese Society for the Promotion of Science at the Fujita Laboratory, Tokyo Institute of Technology, Tokyo, Japan. From 2008 to 2012 she has been an associate professor at Technical University of Munich. Since 2013 she is TUM Liesel Beckmann Distinguished Professor and has the Chair of Information-oriented Control in the Department of Electrical Engineering and Information Technology at Technical University of Munich. Her main research interests include cooperative, distributed and networked control with applications in human-robot interaction, multi-robot systems, and general robotics. She has published more than 150 papers in international journals, books and refereed conferences. Dr. Hirche has served on the Editorial Boards of the IEEE Transactions on Control Systems Technology and the IEEE Transactions on Haptics. She has received multiple awards such as the Rohde & Schwarz Award for her PhD thesis in 2005, the IFAC World Congress Best Poster Award in 2005 and together with students Best Paper Awards of IEEE Worldhaptics and IFAC Conference of Manoeuvring and Control of Marine Craft in 2009.